^{3}H MAS NMR:
A New Approach to Interatomic Distance Measurement

Alexander K.L. Yuen[†], Olivier Lafon[‡], Thibault Charpentier[*,‡], Myriam Roy[†], Francine Brunet[‡], Patrick Berthault[‡], Dimitrios Sakellariou[‡], Bruno Robert[§], Sylvie Rimsky[⊥], Florence Pillon[†], Jean-Christophe Cintrat[†], Bernard Rousseau[*,†]

CEA, iBiTecS, Service de Chimie Bioorganique et de Marquage, F-91191 Gif sur Yvette, France

CEA, iBiTecS, Service de Bioénergétique, Biologie Structurale et Mécanismes, F-91191 Gif sur Yvette, France

CEA, IRAMIS, SIS2M, Laboratoire Structure et Dynamique par Résonance Magnétique, F-91191 Gif sur Yvette, France

LBPA, CNRS, ENS de Cachan, 61, avenue du Président Wilson, F-94235 Cachan, France

---

Supporting Information

I. Synthesis of molecular probes for ^{3}H–^{3}H distance measurement

A. Compound 1: potassium salt of 3,5-Ditritiobenzoic acid

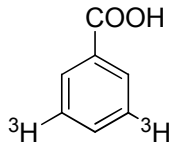

4.31 Å

Prepared from 3,5-dibromobenzoic acid (commercially available), using the general tritiation procedure.
Purified by reverse-phase HPLC (80:20) water: acetonitrile + 0.1% TFA at r.t. Specific activity of 54.8 mCi/µmol (based on GC/MS analysis), being 90% di-labeled, 10% mono-labeled.

4-amino-3-bromobenzoic acid
According to *N-thiazol-2-yl-benzamide derivatives*. PCT int. Appl. WO/2005/039572

4-aminobenzoic acid (1.98 g, 14.4 mmol) was placed under vacuum, flushed with nitrogen and 7 mL of *N*,*N*-dimethylformamide was added. The resulting solution was cooled in an ice

bath and *N*-bromosuccinimide (2.67 g, 15.0 mmol) was added in small portions over a period of 30 min, under positive pressure of nitrogen. The reaction was allowed to warm to room temperature and stirred for 18 h. The reaction was quenched by addition of 15 mL of water, inducing precipitation. The mixture was filtered, washed with water and dried under vacuum, affording the desired compound as a colorless crystalline solid (2.87 g, 95%); R_f 0.25 (3:1 pentane: diethylether); ^{1}H NMR ($CDCl_3$) δ 12.35 (1H, s, CO_2H), 7.85 (1H, d *J* = 2.0 Hz, 3ArH), 7.60 (1H, dd *J* = 8.5, 2.0 Hz, 5ArH), 6.77 (1H, d *J* = 8.5 Hz, 6ArH), 6.10 (2H, s, NH_2).

2-Bromo-4-carboxyphenyldiazonium tetrafluoroborate
According to *J. Chem. Soc. Perkin Trans. 2002, 1126–34*.

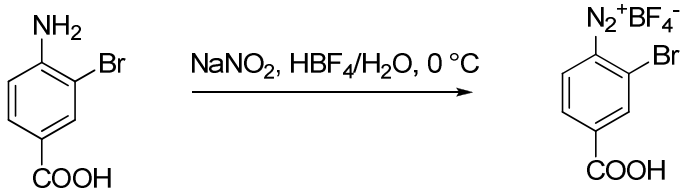

To a solution of 4-amino-3-bromobenzoic acid (501 mg, 2.32 mmol) in 1 mL of aqueous 50% w/v tetrafluoroboric acid and 2.5 mL of water, chilled to 0 °C, was added a solution of sodium nitrite (158 mg, 2.29 mmol) in 1 mL of water, dropwise. The reaction was stirred for 20 minutes, quenched with 100 mL of acetonitrile and the desired product was precipitated upon addition of 1 L of diethyl ether. Filtration and drying under a stream of nitrogen afforded the desired product as a white, crystalline solid (110 mg, 16%); ^{1}H NMR (CD_3CN + 1 drop D_2O) δ 8.70 (1H, d *J* = 8.6 Hz, 6ArH), 8.62 (1H, d *J* = 1.5 Hz, 3ArH), 8.36 (1H, dd *J* = 8.6, 1.5 Hz, 5 ArH).

4-Bromophenyl boronic acid

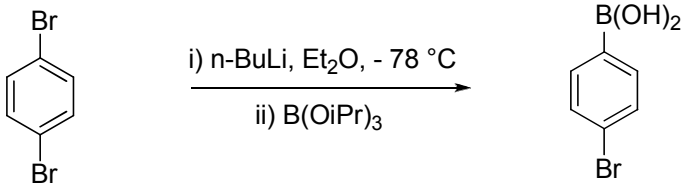

To a flame-dried 500 mL flask, under nitrogen was added 1,4-dibromobenzene (4.72 g, 20.0 mmol) followed by anhydrous diethyl ether (100 mL). The solution was cooled to –78 °C and 1.6 M *n*-BuLi (14 mL, 22 mmol) was added dropwise over 15 min. The reaction was stirred at –78 °C for 1 h then allowed to warm to r.t. over the course of 1 h, then rechilled to –78 °C. Triisopropylborate (7 mL, 30 mmol) was added and the reaction was stirred for a further 15 min and allowed to warm to r.t., during which time precipitate formed.
The reaction was cooled to 0 °C, quenched with 1 M hydrochloric acid (50 mL) and diluted with 50 mL diethyl ether (precipitate dissolved). The two phases were separated and the organic phase was washed with water (2 × 30 mL) and brine (20 mL). The resulting aqueous phase was extracted with ether (2 × 30 mL) and the combined organic extracts were dried over sodium sulfate, filtered and concentrated *in vacuo*, affording 3.88 g of an off-white solid. Colored impurities were removed by trituration with hot pentanes (3 × 30 mL). Recrystallization from water with hot filtration afforded the desired material as a crystalline solid (3.23 g, 80%); ^{1}H NMR (400 MHz, MeOD + 1 drop DCl) δ 7.61 (2H, d *J* = 8.4 Hz, 2,6-

ArH), 7.48 (2H, d J = 8.5 Hz, 3,5ArH); ^{13}C NMR (100 MHz, MeOD + 1drop DCl) δ 136.7, 131.7, 125.8, C *ipso* to B not observed; MS (ESI, negative ion) *m/z* 215 ([({^{81}Br}M+MeOH)–H]$^-$, 100%), 213 ([({^{79}Br}M+MeOH)–H]$^-$, 88%).

2,4'-Dibromobiphenyl-4-carboxylic acid
Adapted from *Org. Lett. 2007, 9(15), 2911–14*

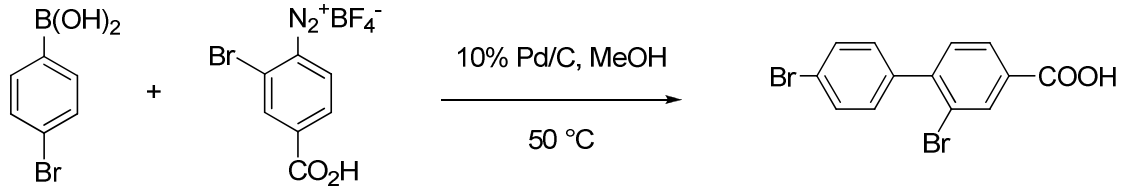

To a dry flask were added 4-bromophenylboronic acid (55.2 mg, 0.28 mmol), 2-bromo-4-carboxyphenyldiazonium tetrafluoroborate (110 mg, 0.35 mmol) and 10% w/w palladium on charcoal (24.5 mg, 23 µmol Pd). The contents were placed under vacuum, repressurized with nitrogen and 3 mL of methanol was added. The reaction was stirred at 50 °C for 1 h, allowed to cool to room temperature, filtered through a Millex^{TM} PTFE syringe filter, washing with methanol (3 × 3 mL), and the solvent was removed. The crude material was purified by semi-preparative HPLC; Zorbax C18, 9.6 mm × 25 cm; eluting with water: acetonitrile: trifluoroacetic acid (60:40:0.1) at 2 mL/min; detected at 220 nm UV; affording the desired product as a white solid (12.4 mg, 12.4%);
^{1}H NMR (CD_3OD) δ 8.15 (1H, app t J = 2.0 Hz, 3ArH), 8.0 (1H, m, 5ArH), 7.75 (1H, m, 6ArH), 7.40 (4H, app t J = 7.9, 2',3',5',6' ArH).

B. Compound 2: potassium salt of 2,4'-Ditritiobiphenyl-4-carboxylic acid

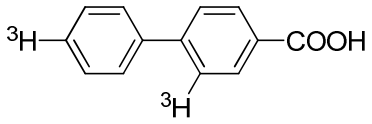

6.0 Å

Prepared from 2,4'-dibromobiphenyl-4-carboxylic acid, using the general tritiation procedure.

275 mCi were purified by reverse-phase HPLC (65:35) water: acetonitrile + 0.1% TFA at r.t. Specific activity of 54 mCi/µmol (based on GC/MS analysis), being 87% di-labeled, 13% mono-labeled.

4,4'-Dibromobiphenyl-2-carboxylic acid

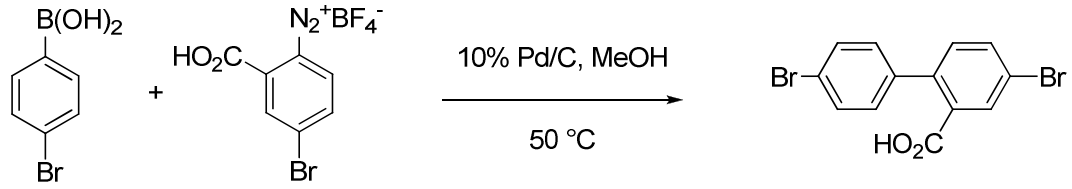

See procedure for 4,4'-dibromobiphenyl-2-carboxylic acid synthesis.

Compound 3: potassium salt of 4,4'-Ditritiobiphenyl-2-carboxylic acid

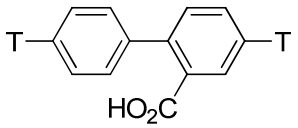

9.4 Å

Prepared from 4,4'-dibromobiphenyl-2-carboxylic acid, using the general tritiation procedure.

100 mCi were purified by reverse-phase HPLC (50:50) water: acetonitrile + 0.1% TFA at r.t. Specific activity of 54.5 mCi/μmol (based on GC analysis), being 88% di-labeled, 12% mono-labeled.

Methyl 2,5-diiodobenzoate

Procedure from *Chemistry & Industry 5th November 1990, p708.*

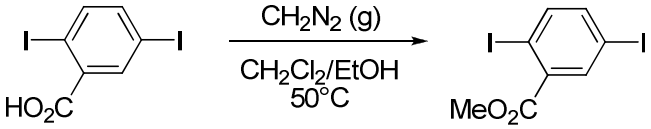

A solution of 2,5-diiodobenzoic acid (1.00 g, 2.67 mmol) in dichloromethane (20 mL) and absolute ethanol (2 mL) was chilled to 0°C. An excess of diazomethane (15.9 mmol in theory) was generated in a separate flask by dropwise addition of concentrated aqueous sodium hydroxide to Diazald™ (5.29 g) suspended in absolute ethanol (30 mL) and, as the gas formed, it was bubbled through the rapidly stirred reaction mixture, carried by a stream of nitrogen gas. Upon completion of addition, the reaction mixture was concentrated under a stream of nitrogen and purified by passage through a 5 cm column of silica, eluting with dichloromethane, affording and off-white solid (1.00 g, 97%); ^{1}H NMR (400 MHz, $CDCl_3$) δ 8.10 (1H, d, J = 2.2 Hz, 6ArH), 7.69 (1H, d, J = 8.3 Hz, 3ArH), 7.45 (1H, d, J = 2.2, 8.3 Hz, 4ArH), 3.93 (3H, s, OMe).

Methyl 4',4''-dibromo-2,5-diphenylbenzoate

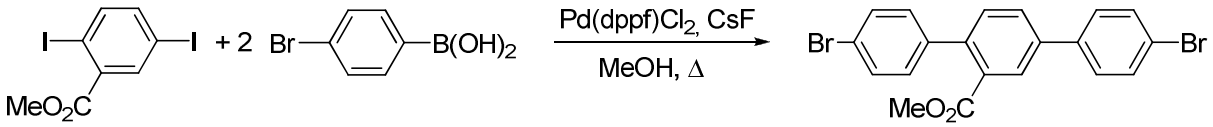

Cesium fluoride (ca 1 g) was quickly weighed into a flask and heated under vacuum to remove water, resulting in a dry white solid (ca 911 mg, 6.00 mmol). Methyl 2,5-diiodobenzoate (388 mg, 1.00 mmol), 4-bromophenylboronic acid (402 mg, 2.10 mmol) and diphenylphoshinoferrocenylpalladium dichloride (41.0 mg, 50.0 μmol) were added to the flask under nitrogen and the mixture was dissolved in dry methanol (10 mL). The reaction mixture was heated at 70 °C overnight then allowed to cool to r.t. and diluted with chloroform (30 mL) and water (10 mL). The two phases were separated, the aqueous phase was further extracted with chloroform (3 × 1 mL) and the combined extracts were dried over sodium sulfate, filtered and concentrated in vacuo. The resulting brown crude solution was filtered through a short plug of silica (using dichloromethane) to remove baseline material and the filtrate was reconcentrated and purified by flash chromatography, eluting with 0–30% dichloromethane (gradient) in hexanes, affording the desired compound as a white solid (230 mg, 50%); ^{1}H NMR (400 MHz, $CDCl_3$) δ 8.04 (1H, dd J = 0.4, 2.1 Hz, 6ArH), 7.72 (1H, dd, J = 2.1, 8.0 Hz, 4ArH), 7.60 (2H, d, J = 8.7 Hz, 2'&6'ArH), 7.54 (2H, d, J = 8.6 Hz, 3"&5"ArH), 7.51 (2H, d, J = 8.8 Hz, 3'&5'ArH), 7.41 (1H, dd, J = 0.4, 8.0 Hz, 3ArH), 7.21

(2H, d, J = 8.6 Hz, 2"&6"ArH), 3.70 (3H, s, OMe); ^{13}C NMR (100 MHz, $CDCl_3$) δ 168.5, 140.5, 139.7, 139.3, 138.4, 132.0, 131.2(8), 121.2(5), 131.0, 130.0, 129.7, 128.6, 128.5, 122.3, 121.7, 52.2; MS (ESI, positive ion) m/z 449 ([{^{81}Br}2M+H]$^+$, 48%), 447 ([{^{81}Br, ^{79}Br }M+H]$^+$, 100%), ([{^{79}Br}2M+H]$^+$, 39%).

4',4''-Dibromo-2,5-diphenylbenzoic acid

Based on *Protecting groups in Organic Chemistry Greene & Wuts.*

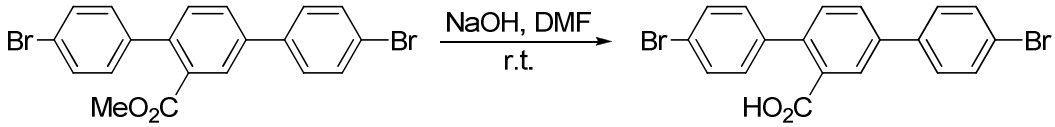

To a solution of the methyl ester (154 mg, 0.34 mmol) in dimethylformamide (3 mL) at r.t., was added a 50% w/v aqueous solution of sodium hydroxide (20 drops). The resulting homogeneous solution was stirred overnight, becoming heterogeneous after 4 h. The reaction mixture was diluted with water (20 mL) and dichloromethane (10 mL) and the pH was adjusted to 2 with conc. hydrochloric acid. The resulting two phases were separated, the aqueous phase was extracted with dichloromethane (2 × 10 mL) and the combined organic extracts were dried over sodium sulfate, filtered and concentrated in vacuo. Purification by flash chromatography (dry loaded sample), eluting with 5% methanol in dichloromethane, afforded 134 mg (90%) of the desired compound as a white solid; ^{1}H NMR (400 MHz, 3:1 $CDCl_3$:CD_3OD) δ 7.92 (1H, d J = 1.9 Hz, 6ArH), 7.56 (1H, dd, J = 2.1, 8.0 Hz, 4ArH), 7.43 (2H, d, J = 8.7 Hz, 2'&6'ArH), 7.37 (2H, d, J = 8.7 Hz, 3'&5'ArH), 7.36 (2H, d, J = 8.5 Hz, 3"&5"ArH), 7.24 (1H, d, J = 8.0 Hz, 3ArH), 7.10 (2H, d, J = 8.5 Hz, 2"&6"ArH); ^{13}C NMR (100 MHz, 3:1 $CDCl_3$: CD_3OD) δ 169.9, 140.2, 139.6, 138.9, 138.2, 131.7, 131.4, 131.0, 130.8, 129.8, 129.2, 128.3, 128.2, 121.8, 121.2; MS (ESI, positive ion) m/z 417 ([{^{81}Br}2M–OH]$^+$, 45%), 415 ([{^{81}Br, ^{79}Br}M–OH]$^+$, 90%), 413 ([{^{79}Br}2M–OH]$^+$, 44%), 336 ([{^{81}Br}M–HOBr]$^+$, 100%), 334 ([{^{79}Br}M–HOBr]$^+$, 95%); MS (ESI, negative ion) m/z 433 ([{^{81}Br}2M–H]$^-$, 60%), 431 ([{^{81}Br, ^{79}Br}M–H]$^-$, 100%), 429 ([{^{79}Br}2M–H]$^-$, 55%).

D; Compound 4: potassium salt of 4',4''-Ditritio-2,5-diphenylbenzoic acid

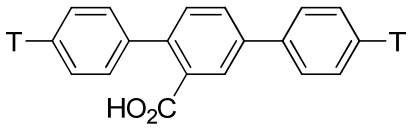

13.8 Å

Prepared from 4',4''-dibromo-2,5-diphenyl-2-benzoic acid, using the general tritiation procedure.

Purified by reverse-phase HPLC (50:50) water: acetonitrile + 0.1% TFA at r.t. Specific activity of 56.0 mCi/μmol (based on GC/MS analysis), being 93% di-labeled, 7% mono-labeled.

General tritiation procedure (This step can be performed by a commercial company)

Tritiation is described for the synthesis of 2,4'-ditritiobiphenyl-4-carboxylic acid:

2,4'-Dibromobiphenyl-4-carboxylic acid (3.00 mg, 8.43 μmol) was dissolved in methanol (1 mL) in a single-neck flask. 10% Palladium on charcoal (5.00 mg, 4.70 μmol Pd) and triethylamine (12 μL, 86.6 μmol) were added to the reaction mixture. The flask was introduced into the glovebox and attached to the tritiation manifold with an attachment collar. The reaction mixture was frozen in liquid nitrogen and placed under high vacuum. Tritium

gas was then introduced and the reaction was allowed to warm to room temperature. Stirring was maintained for 4.5 h under a tritium pressure of 1.36 bars. The reaction flask was then frozen in liquid nitrogen and the tritium atmosphere removed. The reaction mixture was filtered through a 0.45 µm syringe filter, and washed with excess methanol, then evaporated to dryness. Labile tritium atoms were removed by three successive cycles of dissolution in methanol and concentration *in vacuo*. 275 mCi of fixed radioactivity were obtained in the crude material (liquid scintillation counting). Purification by reverse-phase HPLC (65:35) water: acetonitrile + 0.1% TFA provided the pure tritiated product with a specific activity of 54.4 mCi/µmol (based on GC/MS analysis), being 87% di-labeled, 13% mono-labeled.

Specific activity/specific labeling measurement by GC/MS

The acid group of the labeled molecule was esterified affording a more volatile species capable of separation by GC.

Typical procedure on reaction crude:
A solution containing *ca* 3–5 mCi of crude material (in this case the triethylammonium salt) was concentrated to dryness then redissolved in 1 mL of an appropriate solvent (e.g. dichloromethane) and several drops (excess) of trifluoroacetic acid were added to give the free acid. The solution was concentrated to dryness and an excess of ethereal diazomethane (prepared from Diazald™ and stored in ether at –20 °C) was added. The resulting yellow solution, containing the methyl ester, was concentrated under a stream of nitrogen (in hood!) to *ca* 50 µL, transferred to a vial with insert + pierceable cap and immediately analyzed by GCMS.

Confirmation of the desired species and comparative mass spectra for specific activity analysis required the GC/MS of a sample of the corresponding unlabeled methyl ester.

Averaging of the ion chromatogram over the peak of interest and comparison of the abundance of the M^+:$[M–2]^+$ peaks indicated the level of di-labeled to mono-labeled (and non-labeled if $[M–4]^+$ is present) material in the sample.

HPLC purification

Purification was performed on reverse-phase C-18 bonded silica on a preparative column, eluting with a mixture of acetonitrile/water + 0.1% v/v TFA; thus ensuring protonation of the benzoic acid group during purification. Samples were loaded in methanol and in general ≤0.5 mL methanol was tolerated. At a loading volume of more than 1 mL of methanol, significantly poorer separation was observed.
Desired fractions (based on UV detection) were analyzed for chemical and radioactive purity by analytical HPLC, and the identity of each ^{3}H-labeled compound was confirmed by comparison of retention time with that of the corresponding ^{1}H-isotopomer under identical conditions.
Evaporation of the HPLC fractions was followed by redilution to 1 mCi/mL in methanol and storage at –20 °C.
In the case of compound **1** (3,5-ditritiobenzoic acid), significant steam distillation of the acid product was noted upon concentration of the aqueous HPLC fractions. Subsequently, to avoid loss of this material, the HPLC fraction was diluted with cold benzoic acid (in this case a preparation of 1.75 mCi/ mg) before evaporation.

Liquid-state ^{3}H-NMR analysis was typically performed on 10 mCi of the purified material.

General sample preparation for rotor filling (described for compound **2**)

To a solution of 2,4'-ditritiobiphenyl-4-carboxylic acid (60 mCi) in methanol are added biphenyl-4-carboxylic acid (42 mg, 0.21 mmol), potassium carbonate (15 mg, 0.11 mmol, 0.5 eq.) and copper nitrate (aq.) (0.1 mg, 0.2% w/w Cu). The resulting salt solution is concentrated to dryness (at up to 40 °C) and dried overnight under vacuum, over phosphorous pentoxide. Preparing the rotor filling mixture in this way afforded reliable results in terms of sample homogeneity.

For safe filling of the rotor (if not done by the company performing the tritiation), the bench top used and the floor in front of it are covered with taped vinyl film. A balance is positioned on the bench top and an additional vinyl sheet (not fixed) covered with aluminium foil are placed next to it. A large beaker half-filled with methanol, weighing foil, and all necessary spatulas and glassware are prepared and properly arranged on the protected area. The two operators wear protective overalls; a first pair of gloves taped to the overalls' sleeve and a second pair of gloves that can be changed as needed; shoes covers; goggles; and a surgical mask over the mouth and nose. Special care is taken to avoid any air drafts.
A rotor-cap is fitted onto the rotor and an insert is inserted. The rotor is then held vertically with a holder, and a filling funnel is fitted to minimize possible spills. 50 mg of fill mix is weighed onto the weighing foil, then slowly poured into the rotor and packed with a rotor-tamp. When the desired amount of sample is packed in the rotor, the remainder is weighed to determine the exact mass and activity of sample contained into the rotor. The remainder is recovered and any used tools or foil are rinsed with methanol and immersed in the large beaker of methanol.
As a general rule, the gloves of the operator are changed as soon as there is a suspicion of contact with radioactive material. The first operator is the only one handling radioactive material and must not move from the protected area; the second operator oversees the work, providing clean items as needed.
The second insert is then introduced into the rotor and the second cap is fastened. The outside of the rotor is cleaned carefully, the exterior is tested for contamination, and the used gloves, shoe coverings and consumable items are wrapped in the aluminum and vinyl surface coverings and sent for radioactive waste disposal. The immersed glassware is sequentially transferred into 2 beakers containing ethanol and finally properly washed. The surface which was protected by the vinyl and the scale are carefully cleaned with ethanol.
For each rotor filling performed, an excess of 1.85×10^{9} Bq were introduced into the rotor, and *ca* 1×10^{3} Bq was found on the bench-top vinyl sheet; no contamination was ever detected on the bench top or the floor in front of it.

II.NMR Experiments

The NMR data were collected on a Bruker 500WB spectrometer operating at Larmor frequencies of 499.13 MHz and 532.39 MHz for ^{1}H and ^{3}H, respectively. A commercial DOTY XC4 ^{3}H-^{1}H-X triple resonance 4 mm (o.d.) CPMAS probe was used, at a spinning frequency of 8 kHz. This probe was modified (MAS chamber sealed) so that the spinning gas could be monitored by a radiation detector. In order to reduce the risk of a rotor crash, Si_3N_4 thick wall rotors were used. In addition, the sample volume was reduced by employing inserts so as to ensure high homogeneity of the applied radiofrequency (rf) field.

The two pulse sequences used to measure interatomic distances are depicted in Figure S1. ^{3}H-^{3}H dipolar recoupling is performed by employing a low rf field matched to half the spinning frequency, the so-called HORROR condition [1]. Its strength was determined experimentally for each of the investigated samples, as displayed in Figure S2 for sample **1** (similar curves were obtained for samples **2**,**3** and **4** but with decreasing widths of the resonance condition).

Experimental time for each data point is given in the following table.

Compound	Recycle delay (s)	Number of scans	Time/point (s)
1	4	128	512
2	2	256	512
3	1	1024	1024
4	1	4096	4096

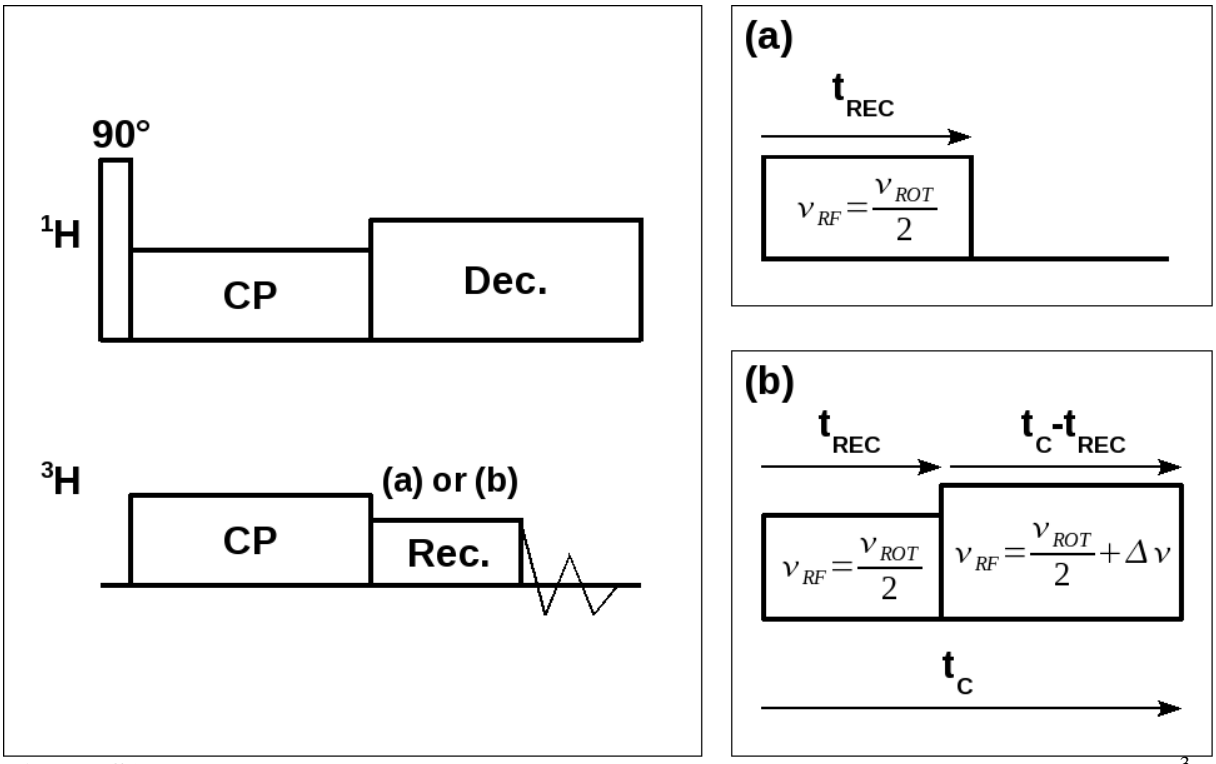

Figure S1: Pulse sequence diagrams used for the distance measurements. (Left panel) ^{3}H magnetization is created using ^{1}H-^{3}H cross-polarization (CP) with a contact time of 120 µs and rf fields of 22 kHz and 38 kHz for ^{3}H and ^{1}H, respectively. Subsequently, the ^{3}H-^{3}H dipolar recoupling is performed during the Rec. period using rf irradiation under HORROR conditions (i.e. rf field strength matched to half the rotor spinning frequency), and a ^{1}H cw decoupling (Dec. period) of about 85 kHz. (Right panel) Two approaches were employed to measure the ^{3}H-^{3}H dipolar oscillation. (a) The recoupling time (t_{REC}) is incremented and followed by the signal detection (Incremental Time version). (b) The recoupling time (t_{REC}) is incremented and followed by a rf irradiation period off the HORROR condition which duration is decremented so as to keep the overall irradiation time (t_C) constant (Constant Time

version). Between 128 to 1024 scans were co-added for each t_{REC} value with a recycle delay ranging from 1s to 4s. Phase cycle as described in [1] have been used.

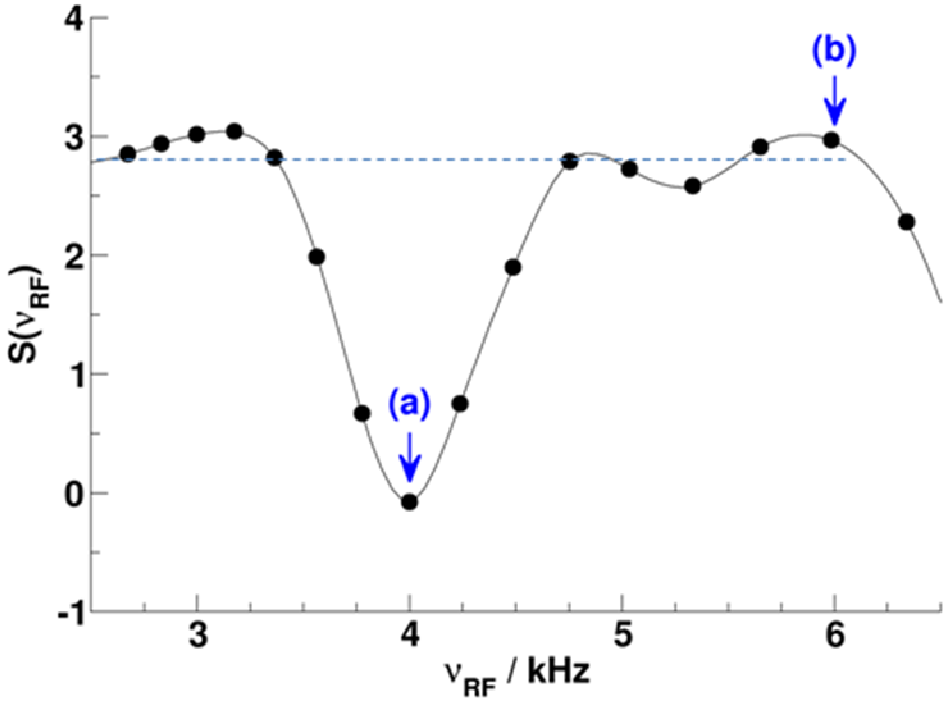

Figure S2(a): For sample **1**, variation of the ^{3}H signal with respect to the rf irradiation field strength of a Rec. period (see Figure S1.(a)) of 500 µs duration. The HORROR condition corresponds to the minimum signal intensity, mark (a). The signal recorded under condition (b) (off HORROR condition) leads to a decaying signal as depicted in Fig. S3 (relaxation in the rotating frame). The choice of the off-HORROR rf field is made within the rf field range as indicated by the dashed line. The fact that within this limited range, i.e. just below and above the HORROR condition, the signal intensity is nearly constant is indicative of a negligible $T_{1\rho}$ variation, as also illustrated by Figure S2(b).

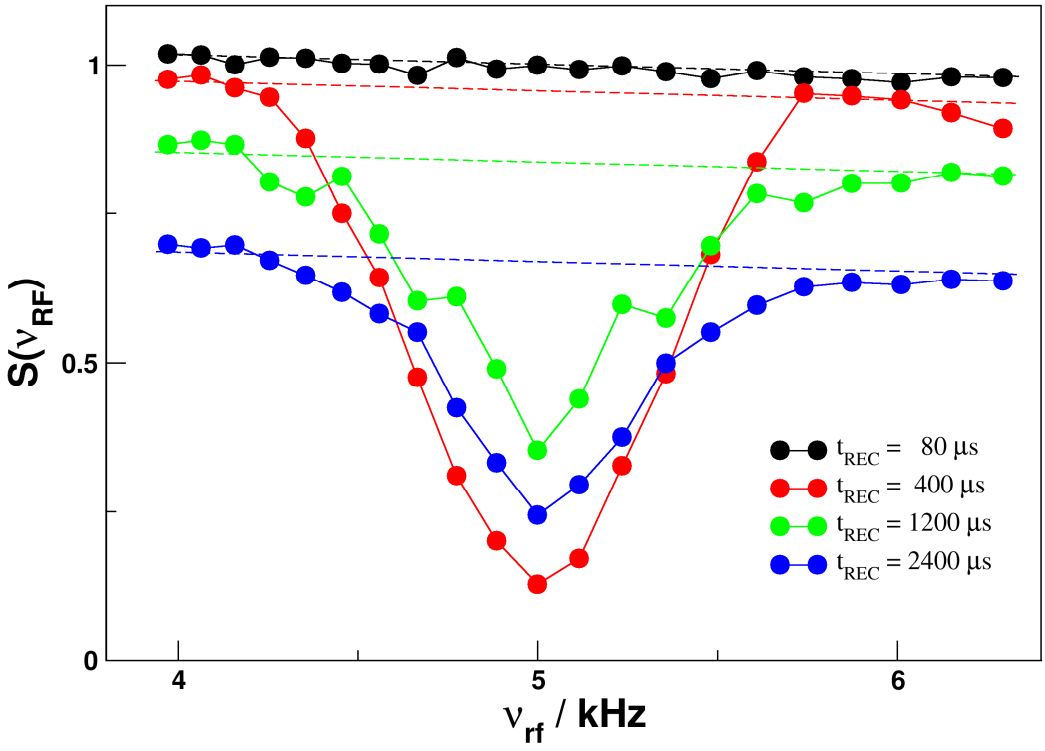

Figure S2(b): For sample **1**, variation of the ^{3}H signal with respect to the rf irradiation field strength of a Rec. period (see Figure S1.(a)) of variable duration (here a spinning frequency of 10 kHz has been used). Dashed lines show that the signal decays, just below and above the HORROR condition are very close, so that within the investigated rf range, $T_{1\rho}$ can be assumed as constant. This defines the rf field range that can be used for the Constant Time (CT) implementation of the HORROR experiment (Fig. S1(b)).

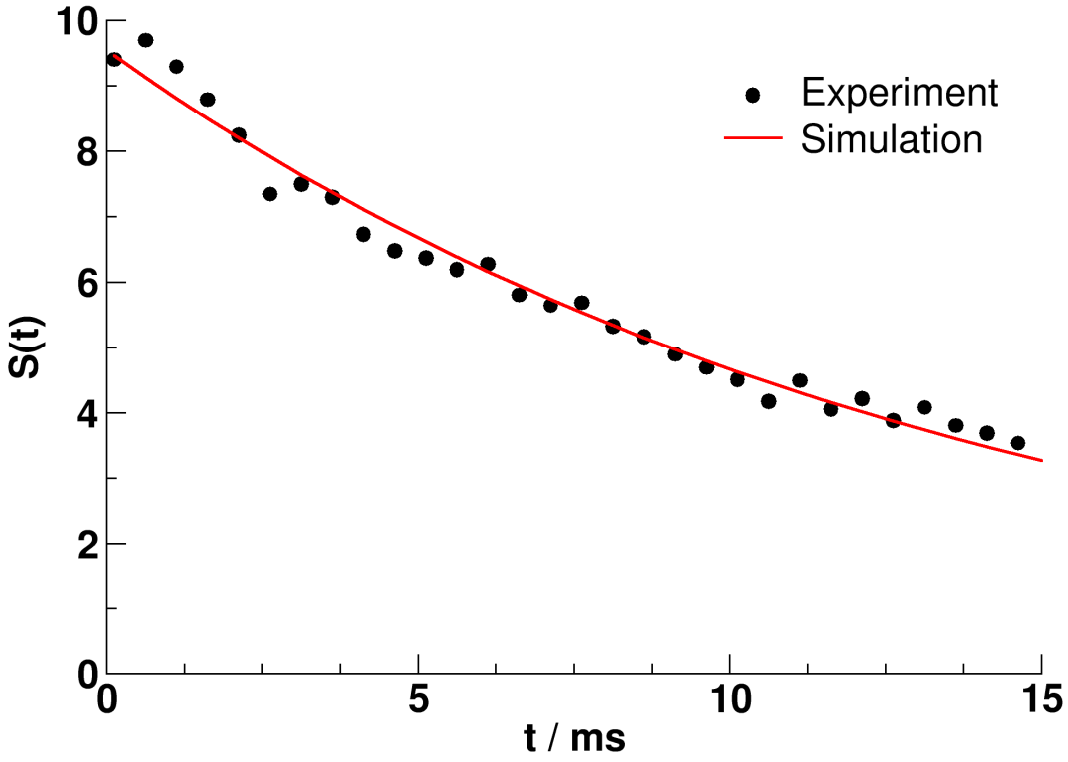

Figure S3: For sample **1**, variation of the ^{3}H signal intensity with respect to the duration of ^{3}H rf irradiation (see Fig. S1(a)) under off-HORROR conditions (see mark (b) in Figure S2). The red line serves as guide for the eyes.

III. NMR Simulations

The dipolar oscillations were simulated using damped signals combining the response of the ^{3}H–^{3}H spin pairs (yielding the dipolar oscillation) and of isolated ^{3}H spins as follows:

$$S_{sim}(t_{rec}) = \left\{A\int S_D(t_{rec};d,\Delta)\mathrm{g}(\Delta)\,d\Delta + B\right\}\times \exp\left(-t_{rec}/T_{1\rho}\right) \quad (1)$$

where $S_D(t_{rec};d,\Delta)$ is the signal of a ^{3}H spin pair with an interatomic distance d, subjected to an rf irradiation strength set at the HORROR condition and at a frequency offset Δ from the center of the ^{3}H line. The latter parameter is introduced to take into account the broad chemical shift distribution, here denoted $g(\Delta)$, owing to the amorphous character of the samples. $T_{1\rho}$ accounts for the relaxation in the rotating frame (see. Fig. S3). With respect to the strength of $g(\Delta)$, the effect of the chemical shift difference between the two tritium sites can be neglected. From liquid state NMR spectra (presented at the end of the present

document), it ranges from 0.2 ppm for compound 2 to 0.04 ppm for compound **4** (and is zero for compound **1**).

For each sample, $g(\Delta)$ was obtained from a fit of the MAS NMR spectrum to a Gaussian distribution. A full width at half maximum (FWHM) of about 800–1000 Hz was observed for all samples. The fact that at a ^{1}H rf decoupling field higher than 50 kHz no line narrowing was observed confirmed that chemical shift distribution was the main mechanism of line broadening. This distribution $g(\Delta)$ causes the response of spin pairs to decrease faster than the single spin response. Additionally, in order to account for other imperfections, mainly the rf field inhomogeneity, a Gaussian broadening over the rf field (FWHM of 100 Hz) was also incorporated in Eq. (1). Those effects have only negligible consequences for compound **1** in which the ^{3}H–^{3}H dipolar interaction is dominant and therefore yields very long-lived dipolar oscillations. For compounds **2**, **3** and **4**, however, because of the decrease of the ^{3}H–^{3}H interactions, Δ and rf inhomogeneity greatly influence the decay of the dipolar oscillations.

The simulations were performed using a custom simulation package, implementing advanced features of the Floquet theory[2].

Determination of the parameters d and $T_{1\rho}$ was performed by minimizing the normalized error function

$$\chi^2 = 100 \times \frac{\int \left(S_{\exp}(t_{rec}) - S_{sim}(t_{rec})\right)^2 dt_{rec}}{\int S_{\exp}^2(t_{rec}) dt_{rec}} \quad (2)$$

where $S_{exp}(t_{rec})$ and $S_{sim}(t_{rec})$ are the experimental and simulated signals, respectively. It is worth noticing in Eq.(1) that during the minimization procedure, for each d and $T_{1\rho}$ values, the parameters A and B are self-consistently determined as $S_{sim}(t_{REC})$ is linearly dependent upon A and B. d and $T_{1\rho}$ are therefore the only two parameters of the fit, so that minimum of χ^2 can be easily obtained from an exhaustive calculation for a range of d and $T_{1\rho}$ values, as depicted in Fig. S4. To determine the level of accuracy of the distance measurement, we chose as a criterion the distance deviation leading to a twofold increase of χ^2 from its minimum. For sample **1**, this was obtained for distances d=4.33 Å and 4.37 Å (see Fig. S4), yielding a 0.02 Å accuracy. As shown in Fig. S4 (right panel), no correlation between the two fit parameters is observed.

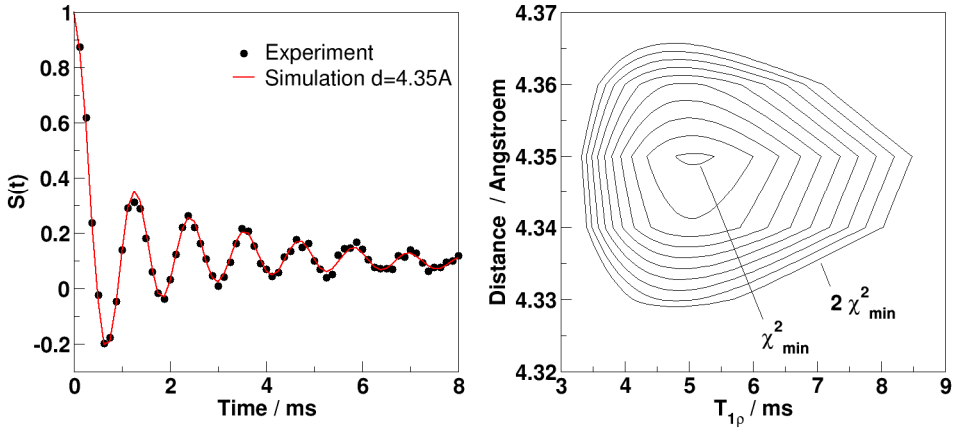

Figure S4: For compound **1**. (Left panel) experimental (circles) and simulated (solid line) variations of the ^{3}H signal intensity under HORROR conditions. (Right panel) Variation of the error function (Eq.(2)) with respect to the two fit parameters d and $T_{1\rho}$. The error is minimized for the values d=4.35Å and $T_{1\rho}$=5.1 ms.

For sample **2** (Fig. S5), the best fit using Eq. (1) yielded $T_{1\rho}$=4.9 ms and d=5.9 Å with a distance accuracy of 0.1 Å.

For sample **3** (Fig. S6), a slightly modified equation was used in order to account for the non-exponential decrease of the off-HORROR resonance decay:

$$S_{sim}(t_{rec}) = \left\{A \times \int S_D(t_{rec};\Delta) \times g(\Delta)\, d\Delta + B\right\} \times \left\{\exp\left(-t_{rec}/T_1\right) + C\right\} \quad (3)$$

The constant C is in fact representative of a very long decay component, while the B term represents the short decay component. This yielded $T_{1\rho}$=1.3 ms and d = 9.2 Å with a distance accuracy of about 0.3 Å.

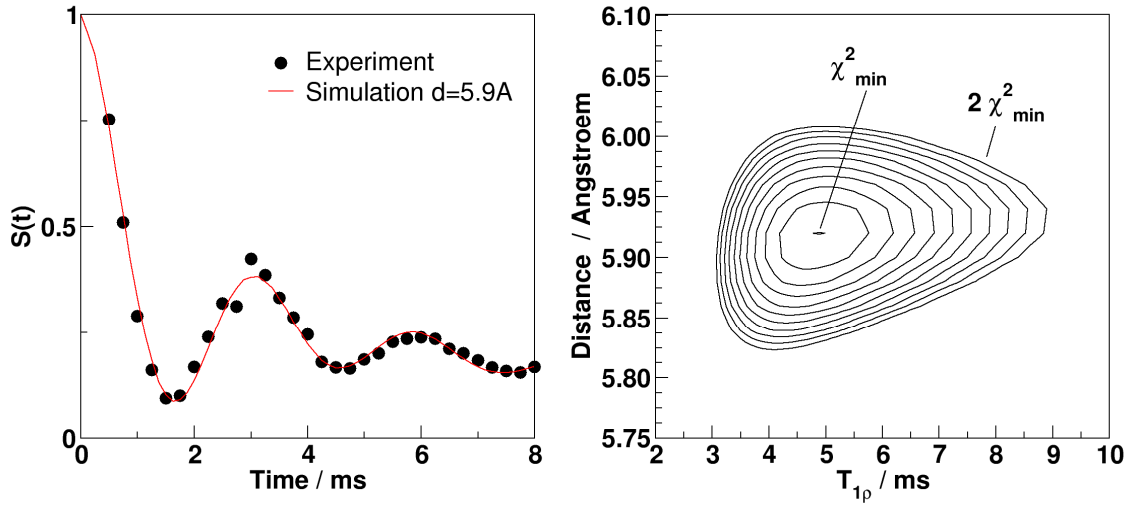

Figure S5: For compound **2**. (Left panel) experimental (circles) and simulated (solid line) variations of the ^{3}H signal intensity under HORROR conditions. (Right panel) Variation of the error function Eq.(2) with respect to the two fit parameters d and $T_{1\rho}$. The error is minimized for the values d=5.92 Å and $T_{1\rho}$=4.9 ms.

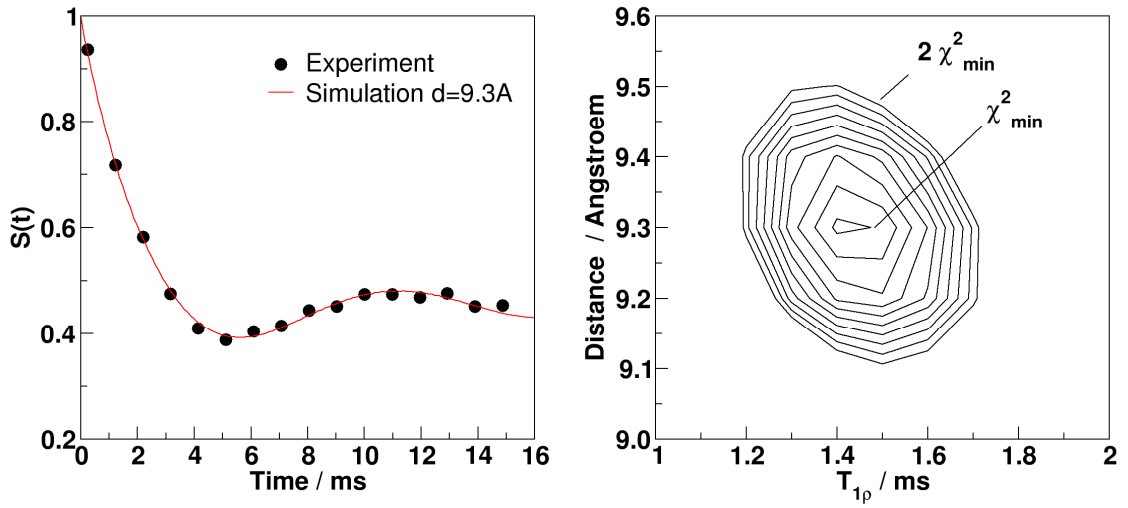

Figure S6: For compound **3**. (Left panel) experimental (circles) and simulated (solid line) variations of the ^{3}H signal intensity under HORROR conditions. (Right panel) Variation of the error function Eq.(2) with respect to the two fit parameters d and $T_{1\rho}$ (C is fixed to its optimized value 1.3). The error is minimized for the values d=9.3Å, $T_{1\rho}$=1.4 ms.

Constant-time HORROR experiments

For compound **4** (13.8 Å) no dipolar oscillations could be observed using the HORROR pulse sequence depicted in Fig.S1a, mainly because of the shortness of the $\mathbf{T_{1\rho}}$ relaxation time. We therefore implemented the pulse sequence using a constant time approach, as depicted in

Fig.S1b. In such a way, the dependence of the measured signal with respect to $\mathbf{T_{1\rho}}$ in Eq. (1) is removed. This yields the new model

$$S_{sim}^{CT}(t_{REC}) = A\int S_D(t_{REC};d,\Delta)\mathrm{g}(\Delta)\,d\Delta + B \quad (4)$$

which is now dependent upon a single parameter d (the ^{3}H-^{3}H distance). This experimental approach was validated comparing the results of the incremental and constant-time sequences on compound **1**. The same oscillations were observed in each case (Figure S7). Fit of the data with Eq. (4) yielded the same value for the extracted distance. This clearly showed that the rf field difference of 2 kHz between the HORROR and off-HORROR irradiation does not induce a significant $\mathbf{T_{1\rho}}$ difference (as can also be inferred from Fig.S2). The rf field difference has to be chosen as the smallest one to ensure negligible $\mathbf{T_{1\rho}}$ variation. But the longer the distance, the smaller it can be, as a result of the narrower dip of the HORROR condition (Fig. S2). For compound 4 (Figure S8), a constant time of 16 ms was chosen (this value has to be chosen in compromises between the signal intensity reduction due to T1ρ and the dipolar oscillations) and a rf field difference of about 200 Hz. For such a small difference, $T_{1\rho}$ variation can be fully neglected. The plot of the error function versus the distance d exhibits a rather flat minimum between 13.2 Å and 15.8 Å. Applying the criterion given above leads to an estimated distance of 14.4 Å with a 2.2 Å accuracy.

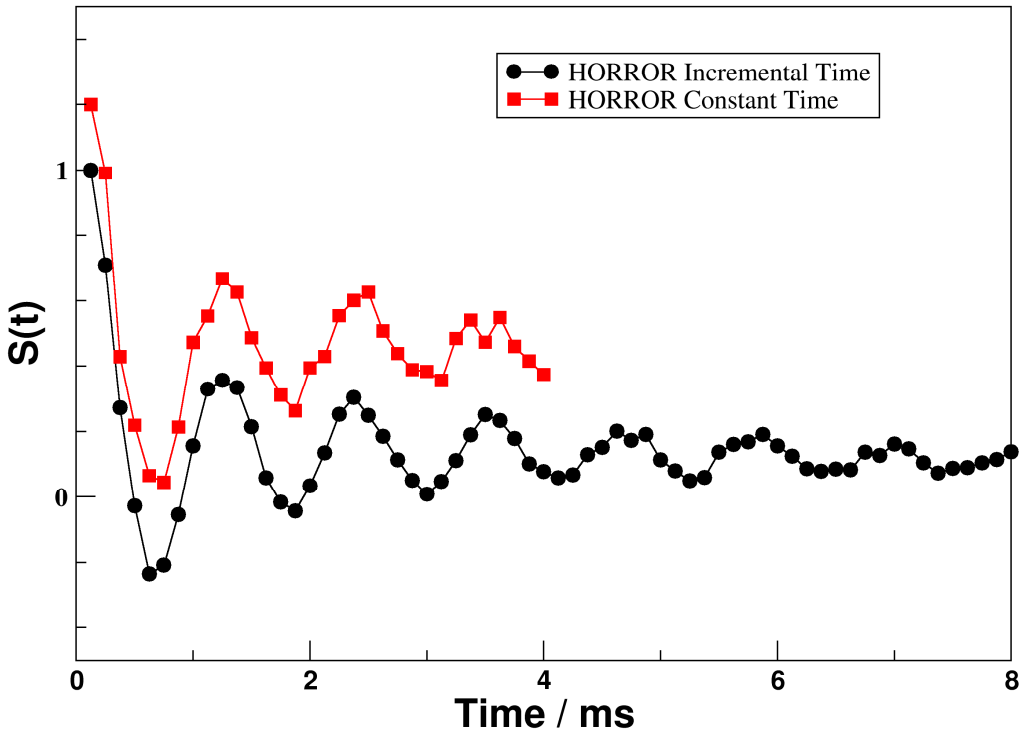

Figure S7: For compound **1**, comparison between the variations of the ^{3}H signal under rf irradiation at the HORROR conditions (here, 4kHz rf irradiation) obtained by incrementing the overall rf irradiation duration (circles, sequence Fig. S1a) and by the constant time

approach (squares, sequence Fig.S1b with off-HORROR irradiation at 6 kHz); t_c=4ms. For sake of clarity, the CT curve has been shifted upwards.

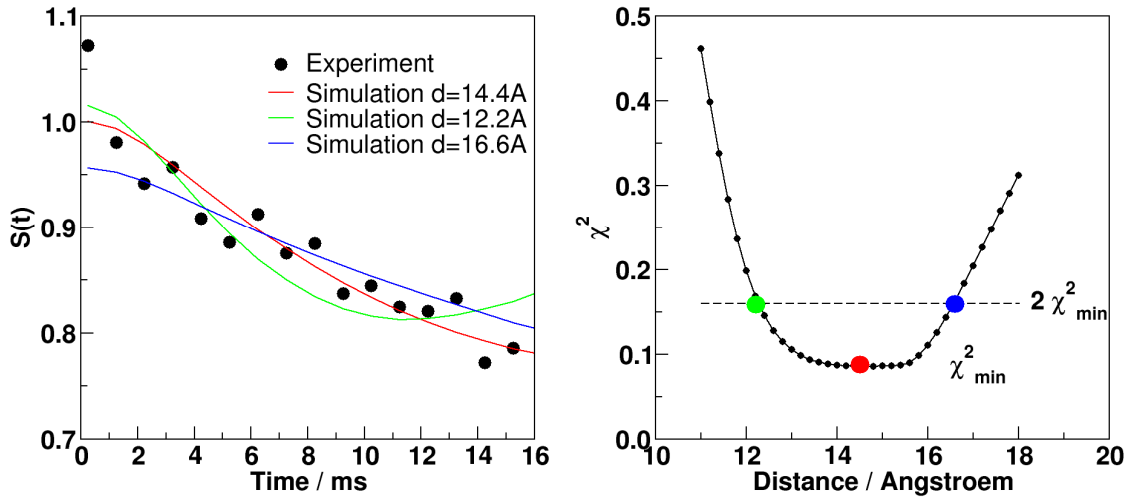

Figure S8: For compound **4**. (Left panel) experimental (circles) and simulated (solid lines) variations of the ^{3}H signal intensity under Constant Time HORROR conditions. (Right panel) Variation of the error function Eq.(2) with respect to the fit parameter *d*. The error minimum is relatively flat for d between 13.2Å and 15.8Å.

(1) Nielsen, N.C.; Bildsøe, H.; Jakobsen, H.J., Levitt, M.H.; *J. Chem. Phys*. **1994**, *101*, 1805–1812.
(2) Charpentier, T.; Fermon, C.; Virlet, J.; *J. Magn. Reson.* **1998**, *132*, 181–190.

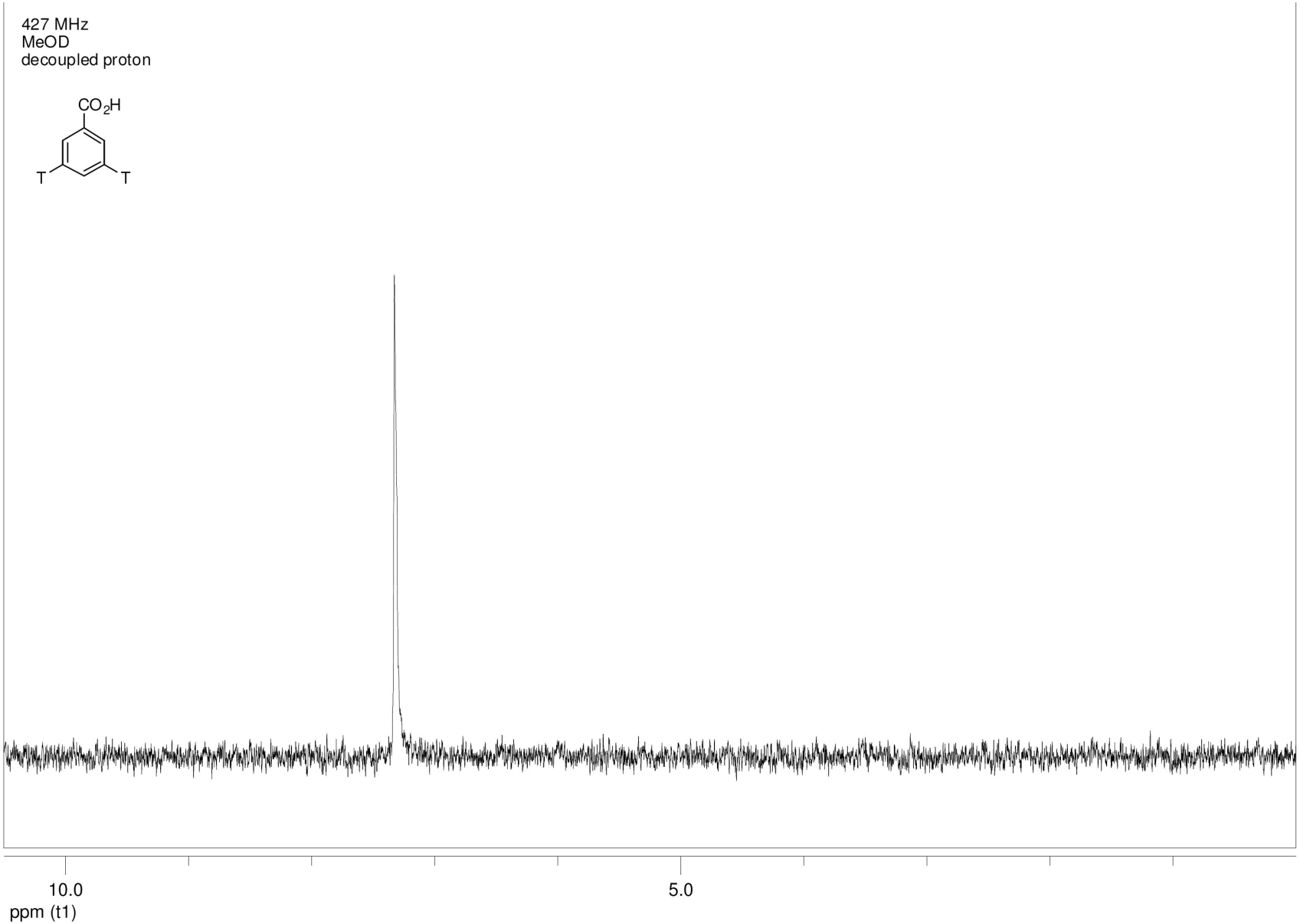
427 MHz
MeOD
decoupled proton
CO2H
T
T
10.0
ppm (t1)
5.0

400 MHz
DMSO

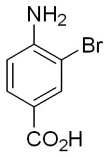

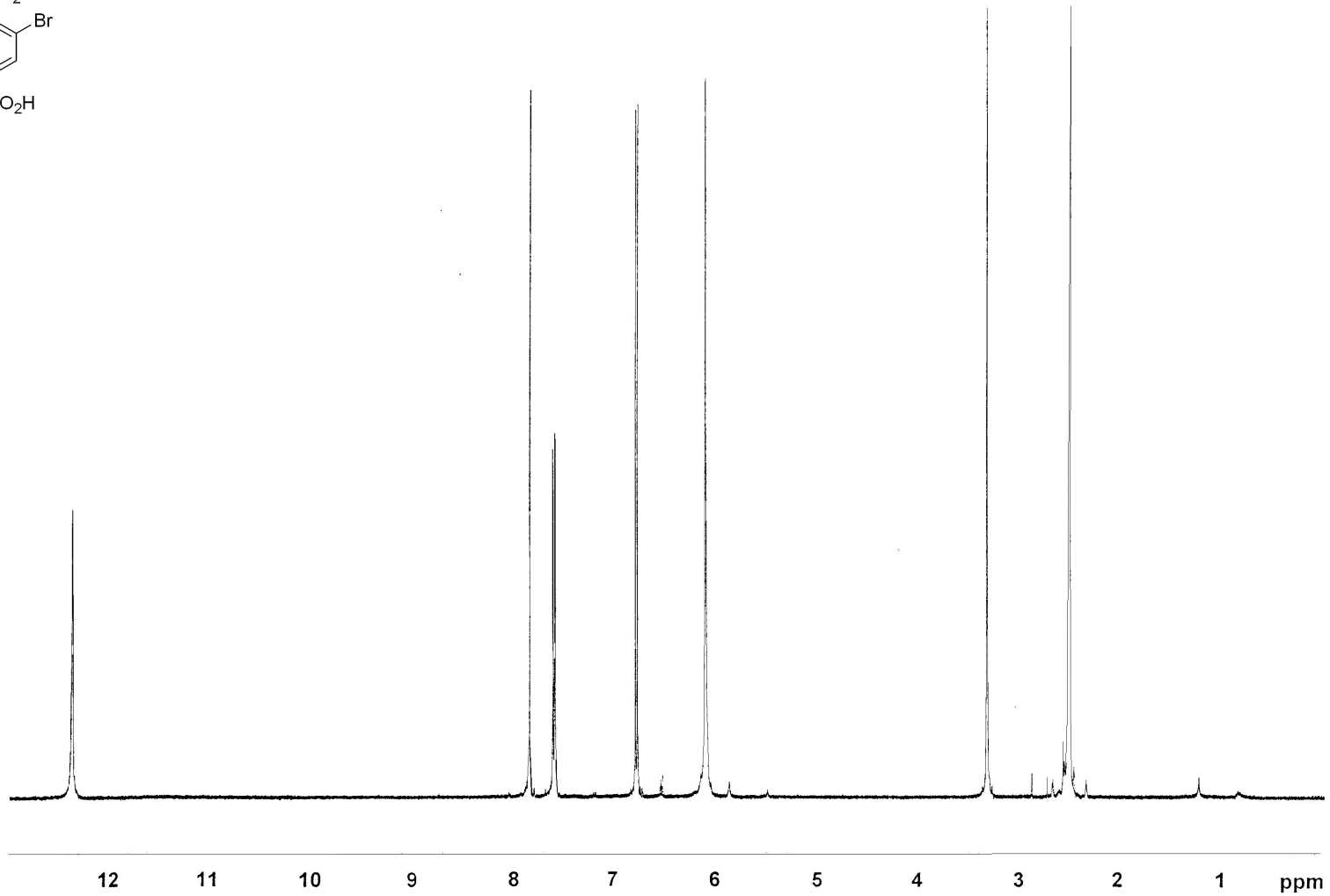

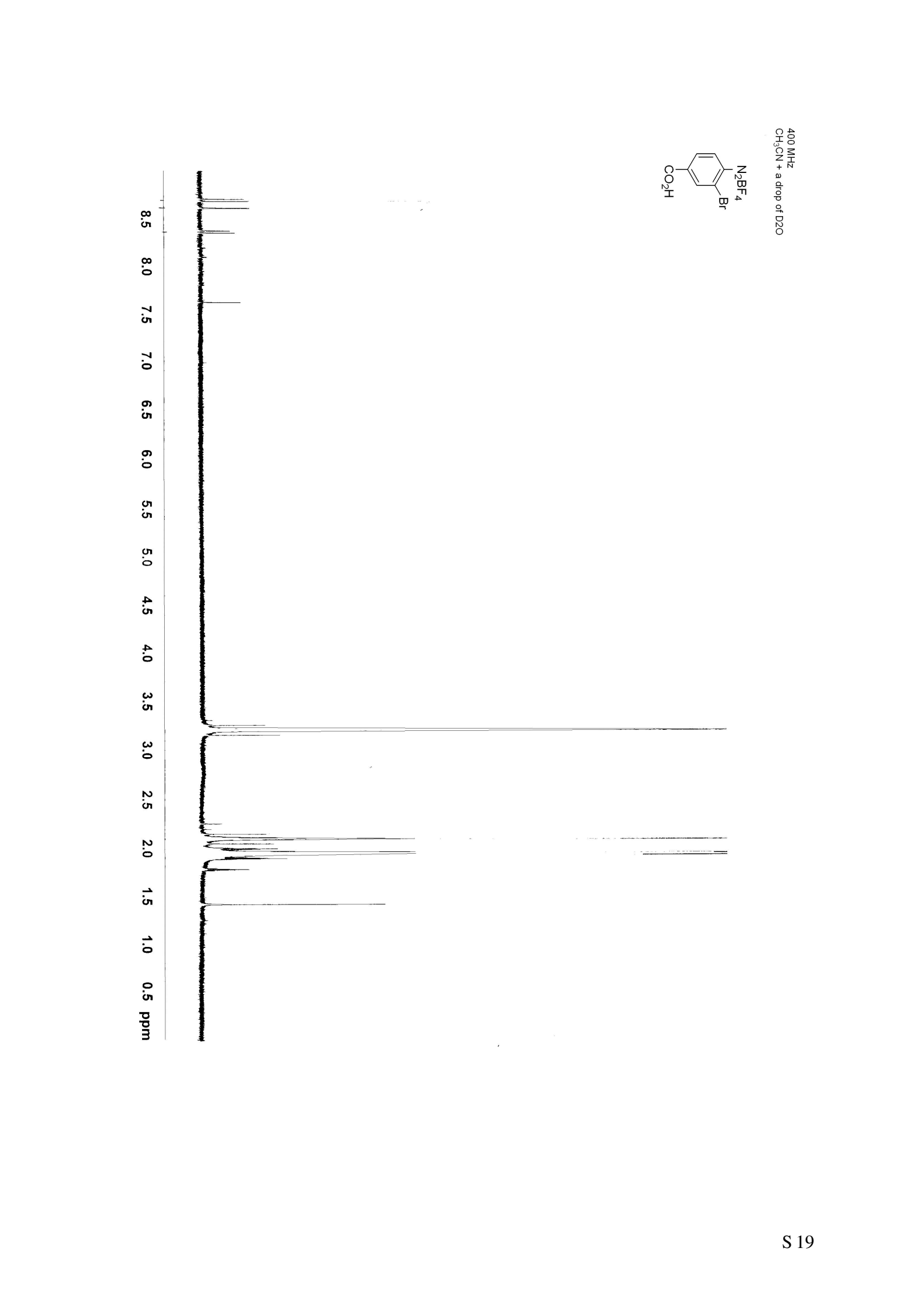
400 MHz
CH3CN + a drop of D2O
N2BF4
Br
CO2H
8.5
8.0
7.5
7.0
6.5
6.0
5.5
5.0
4.5
4.0
3.5
3.0
2.5
2.0
1.5
1.0
0.5
ppm

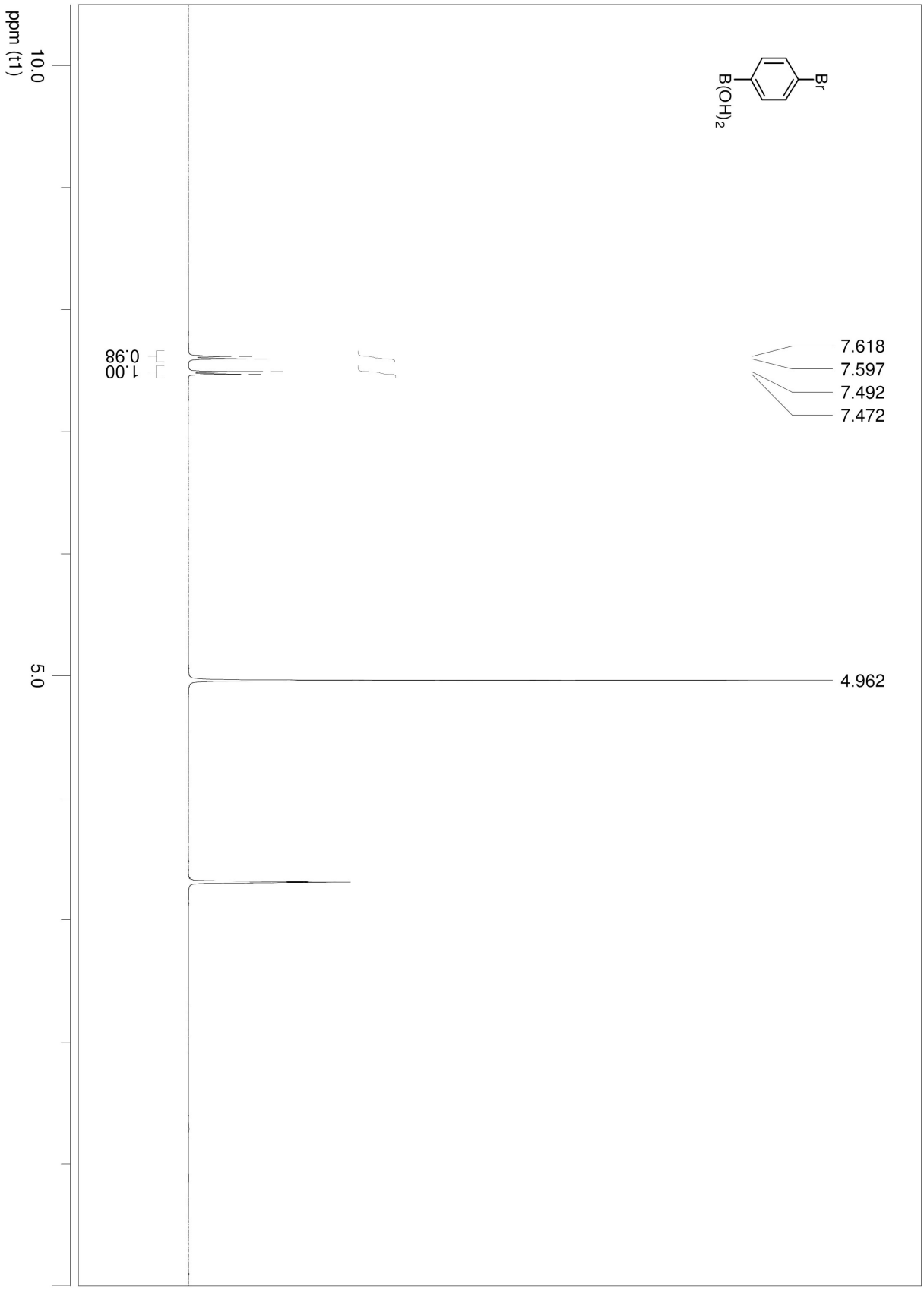
10.0
ppm (t1)
5.0
B(OH)2
Br
0.98
1.00
7.618
7.597
7.492
7.472
4.962

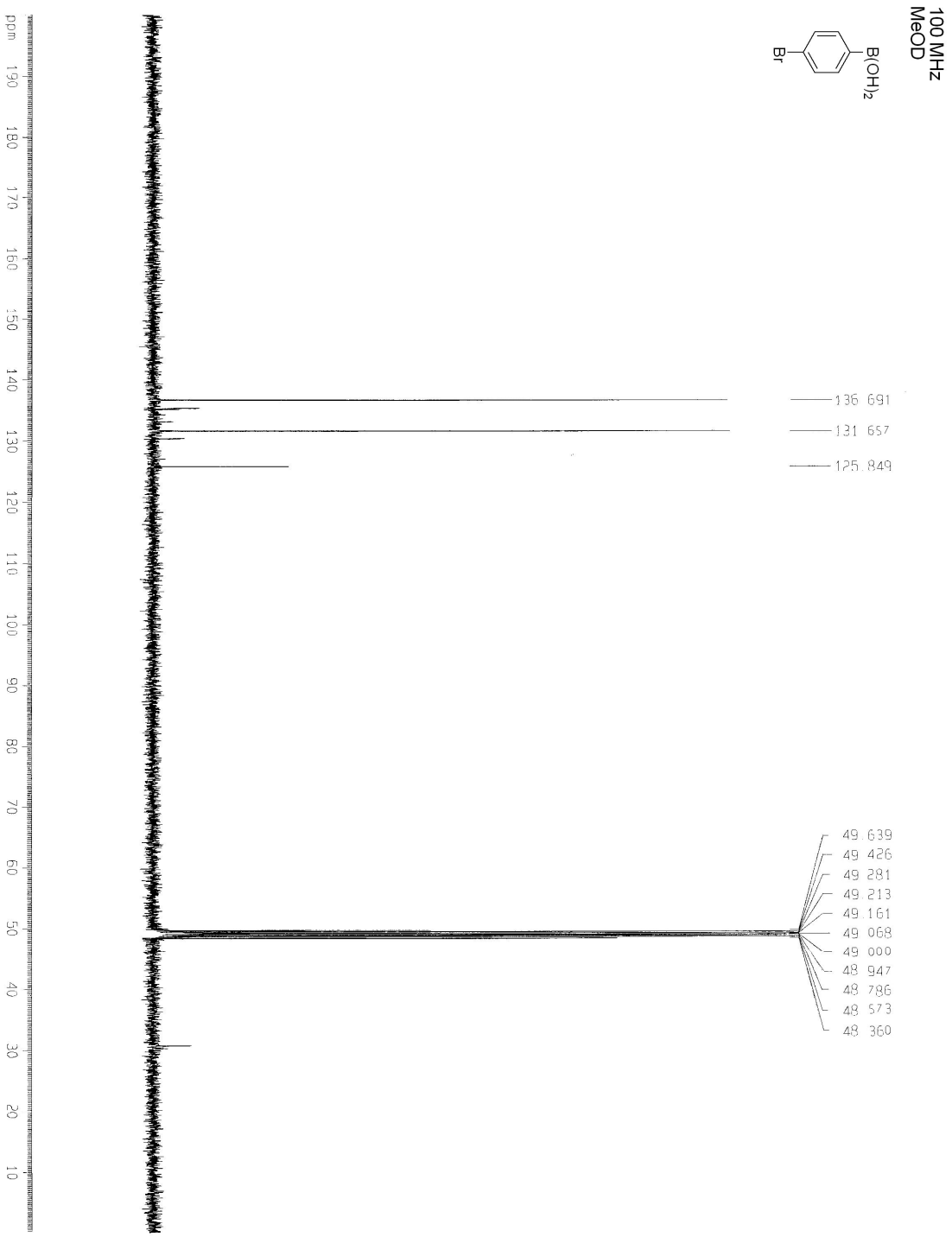
100 MHz
MeOD
Br
B(OH)2
136.691
131.657
125.849
49.639
49.426
49.281
49.213
49.161
49.068
49.000
48.947
48.786
48.573
48.360
ppm
190
180
170
160
150
140
130
120
110
100
90
80
70
60
50
40
30
20
10

400 MHz
MeOD

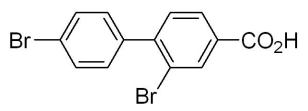

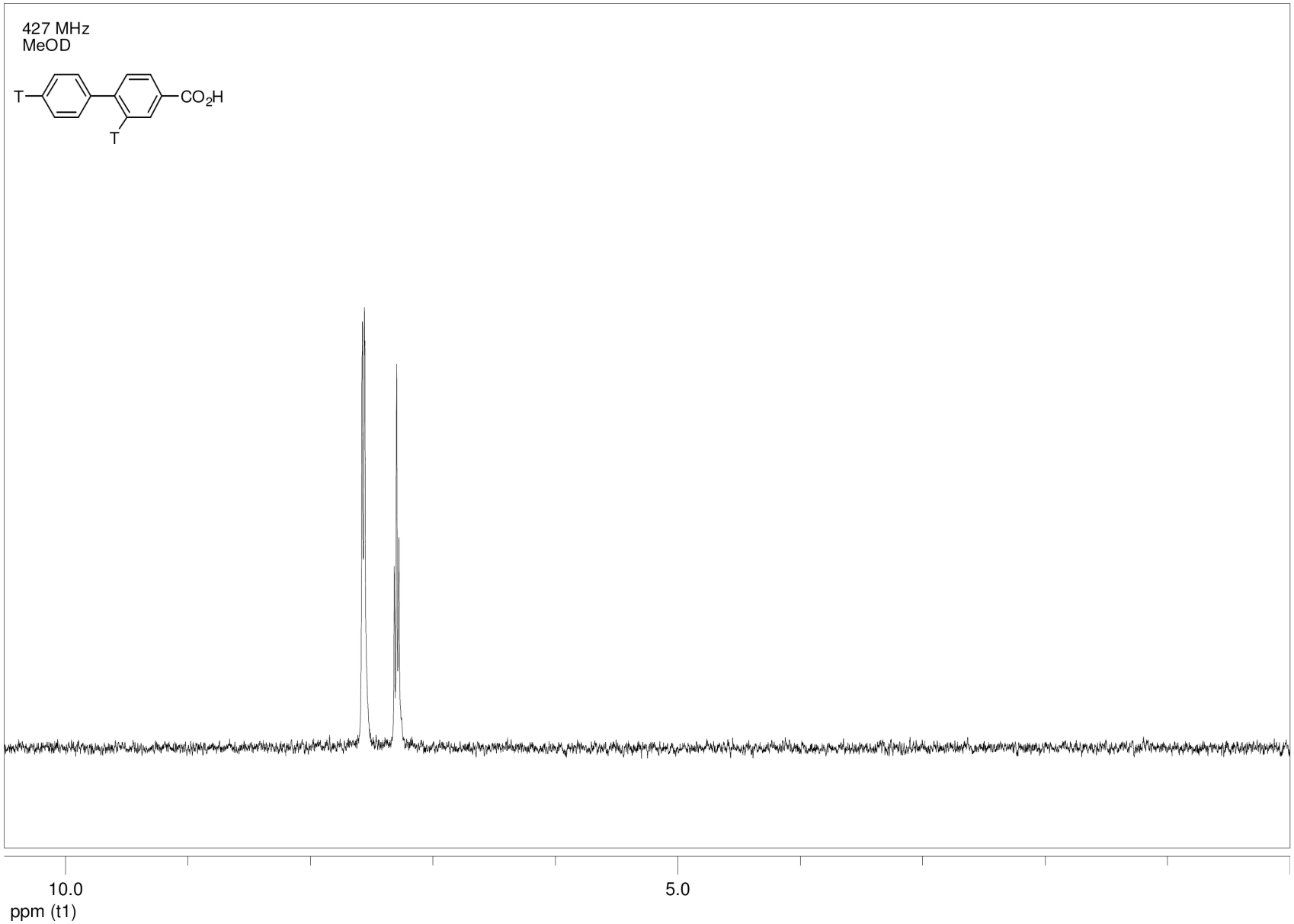
427 MHz
MeOD
T
CO2H
T
10.0
ppm (t1)
5.0

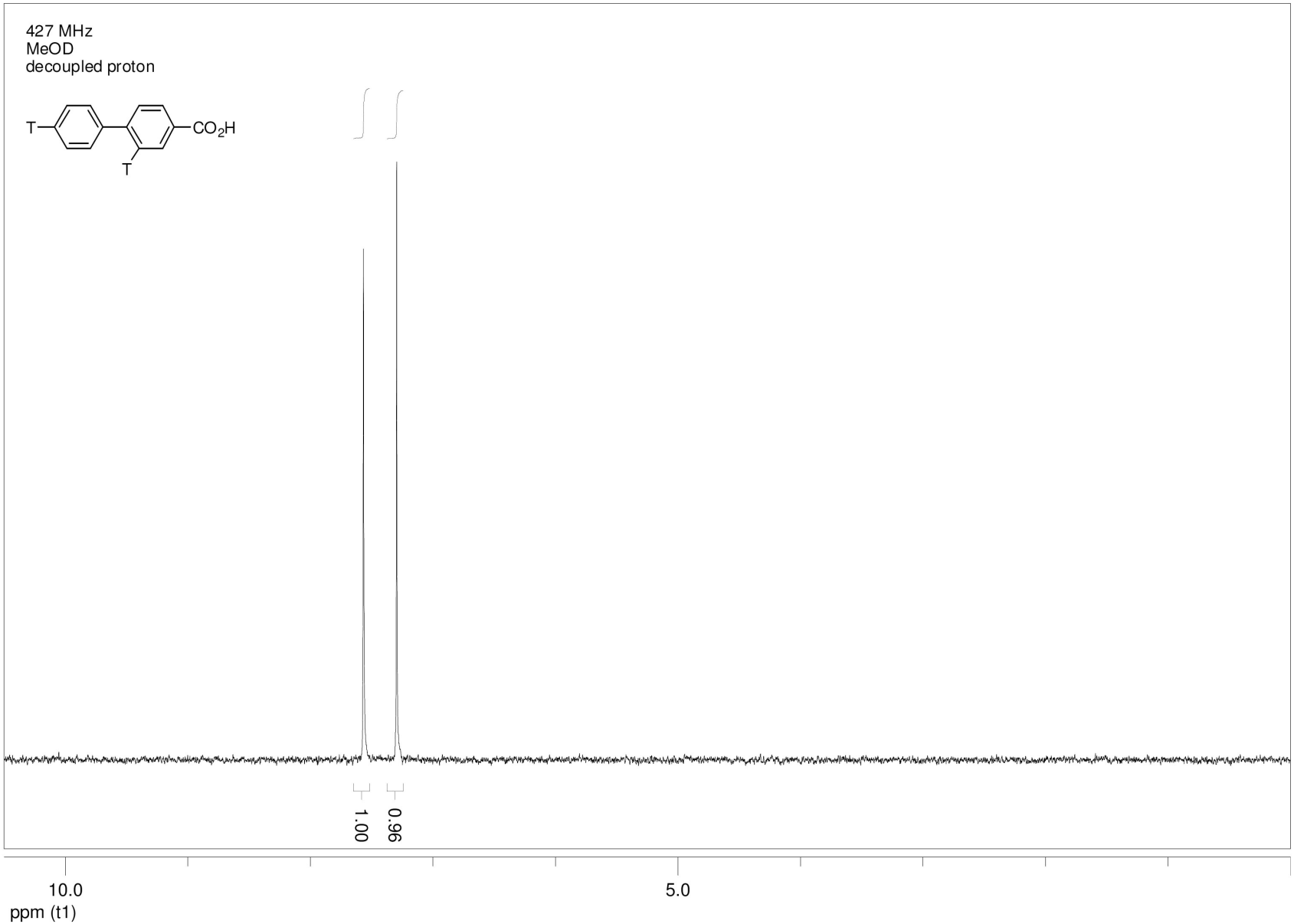
427 MHz
MeOD
decoupled proton
T
CO2H
T
1.00
0.96
10.0
ppm (t1)
5.0

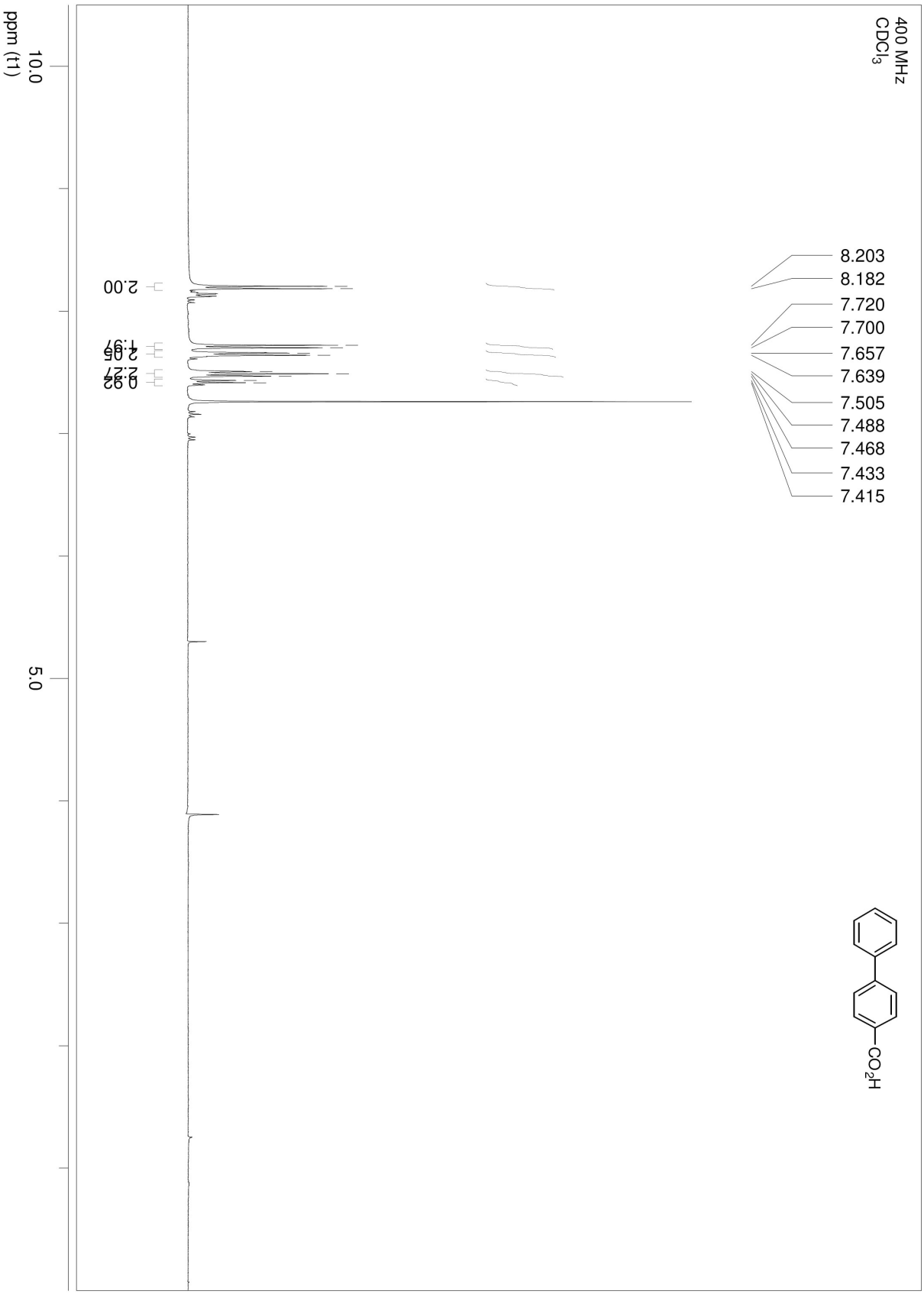
400 MHz
CDCl3
8.203
8.182
7.720
7.700
7.657
7.639
7.505
7.488
7.468
7.433
7.415
2.00
1.97
2.05
2.27
0.92
CO2H
10.0
ppm (t1)
5.0

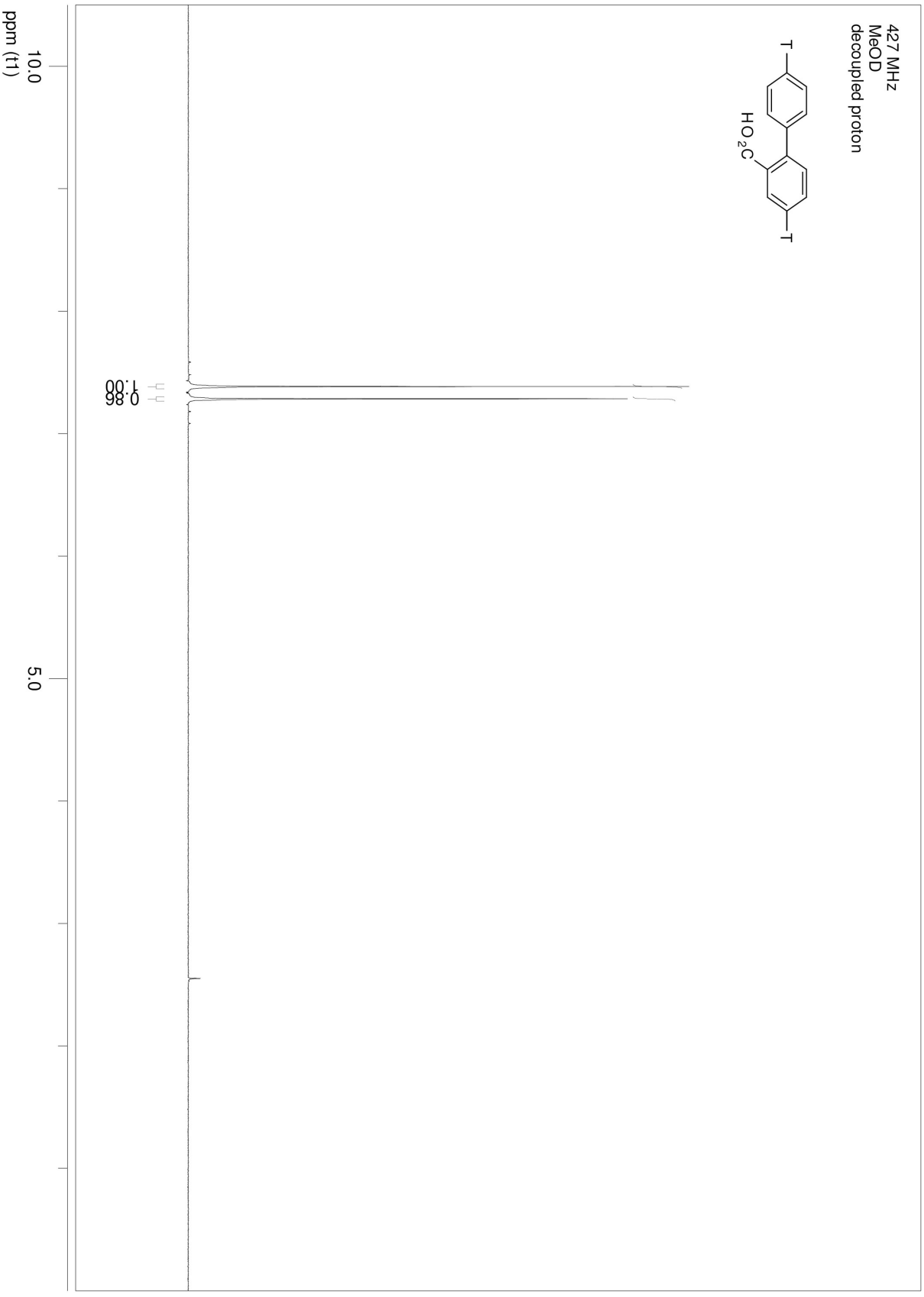
427 MHz
MeOD
decoupled proton
T
HO2C
T
0.86
1.00
10.0
ppm (t1)
5.0

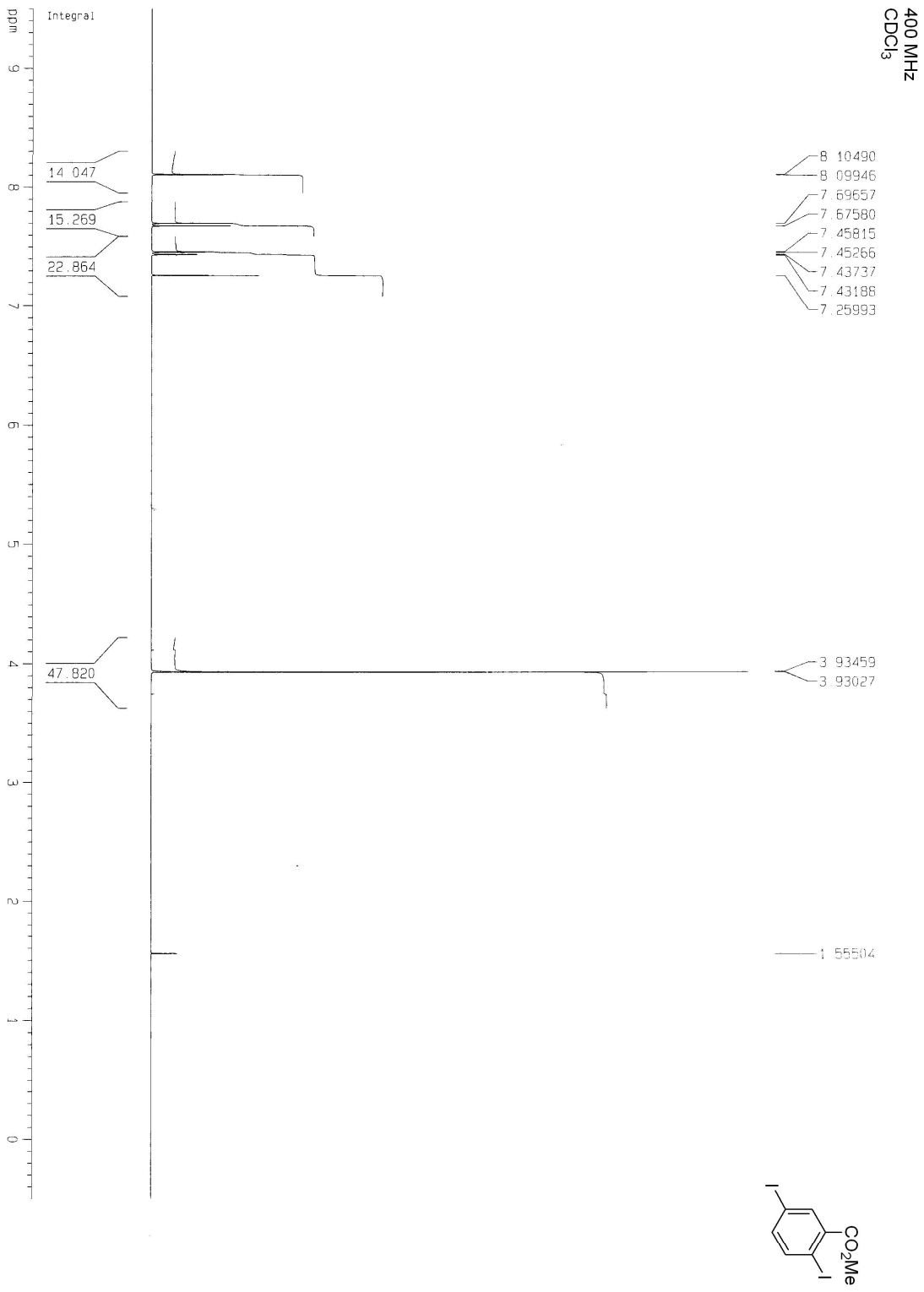
400 MHz
CDCl3
ppm
Integral
14.047
15.269
22.864
47.820
8.10490
8.09946
7.69657
7.67580
7.45815
7.45266
7.43737
7.43188
7.25993
3.93459
3.93027
1.55504
I
CO2Me
I

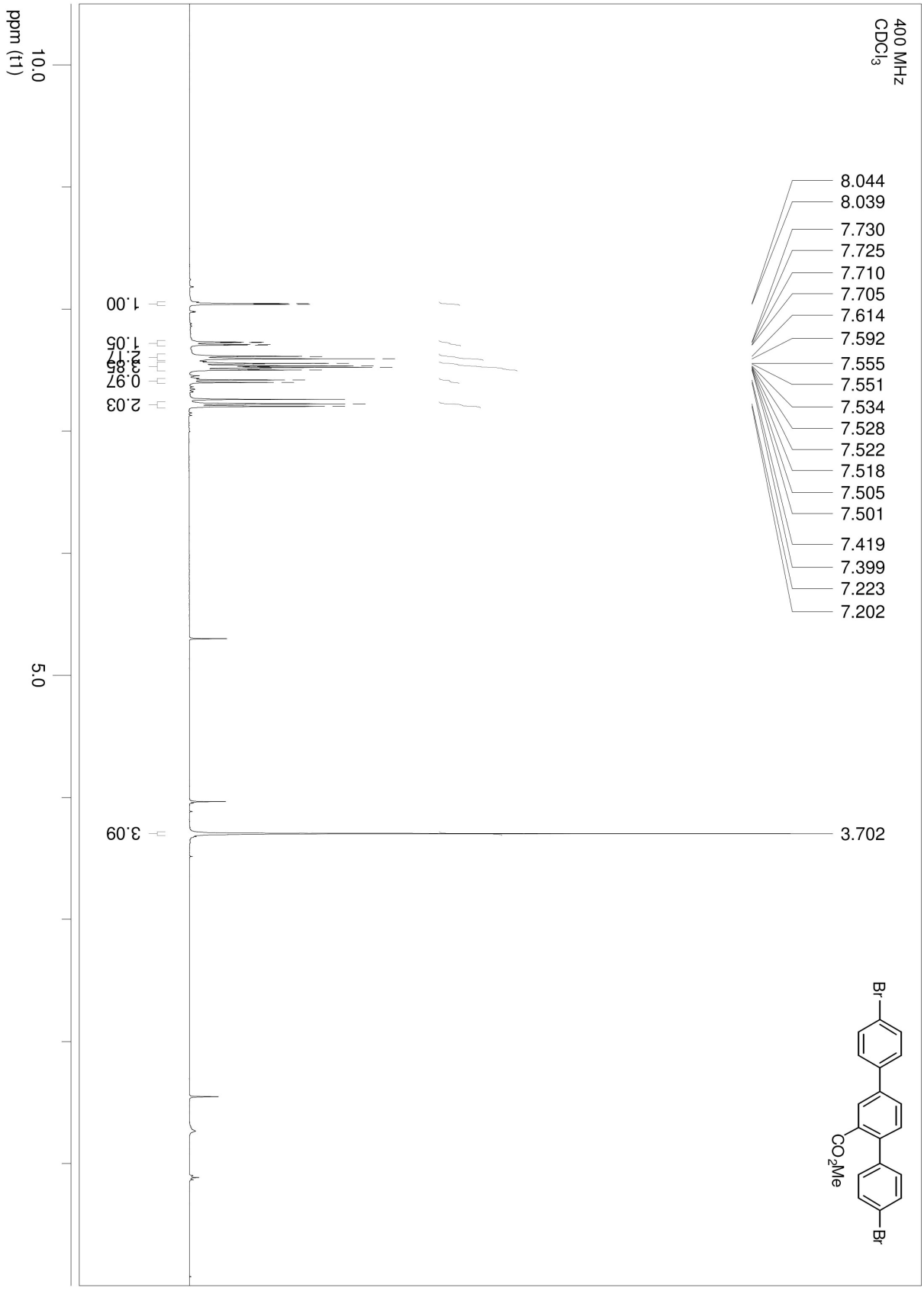
400 MHz
$CDCl_3$
8.044
8.039
7.730
7.725
7.710
7.705
7.614
7.592
7.555
7.551
7.534
7.528
7.522
7.518
7.505
7.501
7.419
7.399
7.223
7.202
3.702
1.00
1.05
2.17
3.85
0.97
2.03
3.09
10.0
ppm (t1)
5.0
Br
CO_2Me
Br

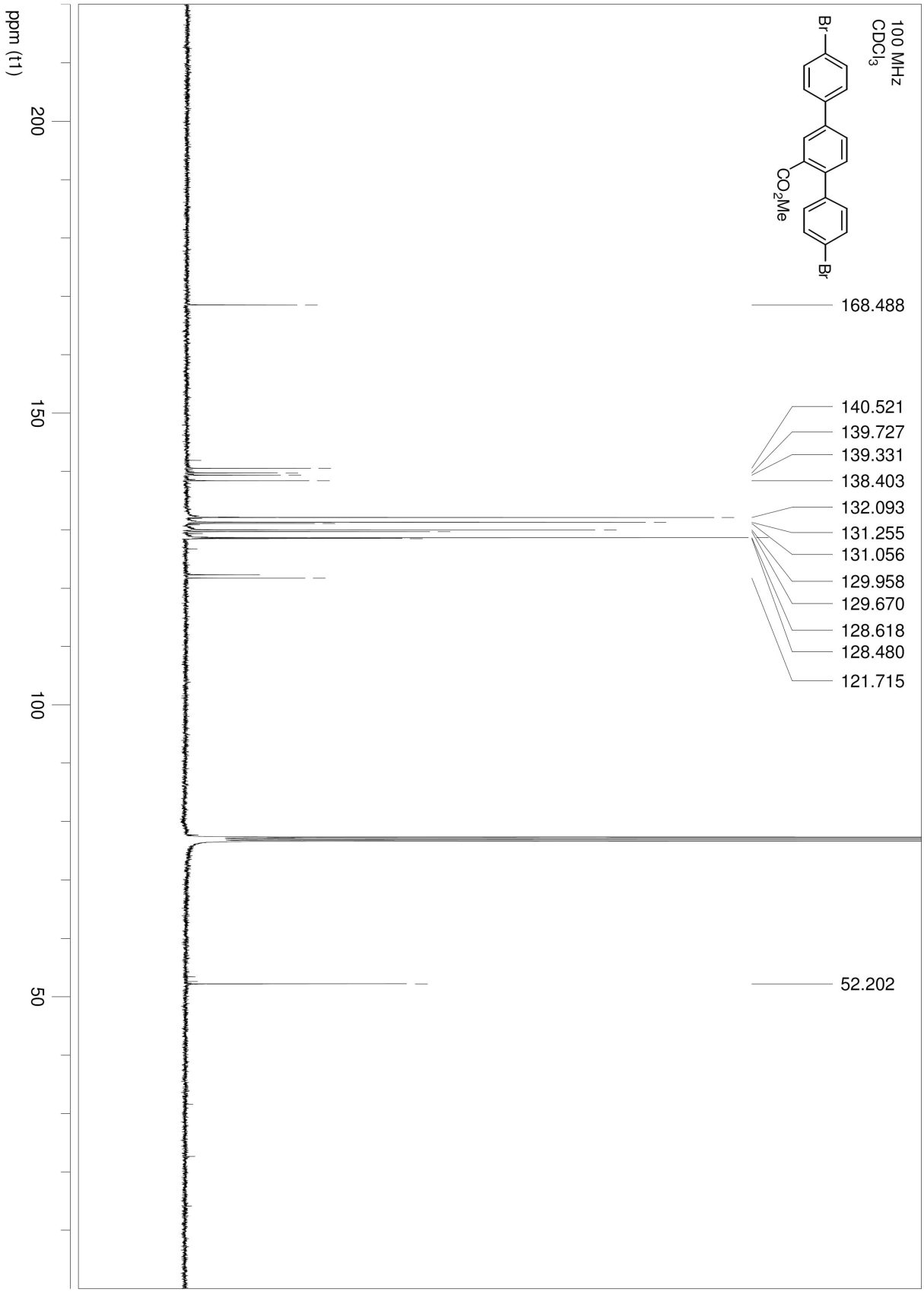
100 MHz
$CDCl_3$
Br
CO_2Me
Br
168.488
140.521
139.727
139.331
138.403
132.093
131.255
131.056
129.958
129.670
128.618
128.480
121.715
52.202
ppm (t1)
200
150
100
50


ppm (t1)
5.0
0.0
1.00
1.07
6.39
1.84
2.10
7.833
7.809
7.460
7.457
7.335
7.329
7.307
7.279
7.260
7.239
7.230
7.175
7.161
7.145
7.132
7.020
7.017
7.000
6.992
6.971
400 MHz
MeOD, CDCl3
Br
CO2H
Br

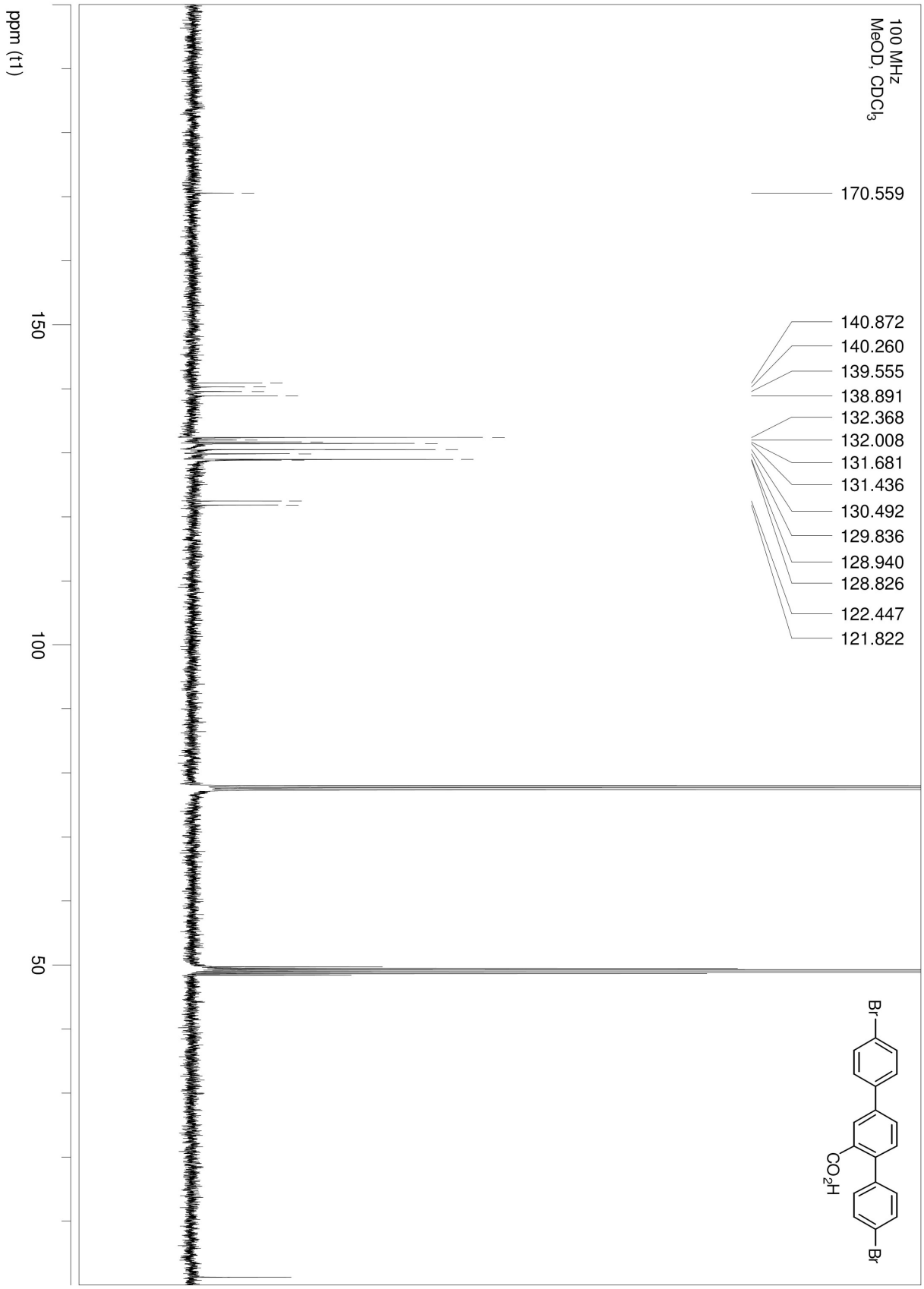
100 MHz
MeOD, $CDCl_3$
170.559
140.872
140.260
139.555
138.891
132.368
132.008
131.681
131.436
130.492
129.836
128.940
128.826
122.447
121.822
150
100
50
ppm (t1)
Br
CO_2H
Br

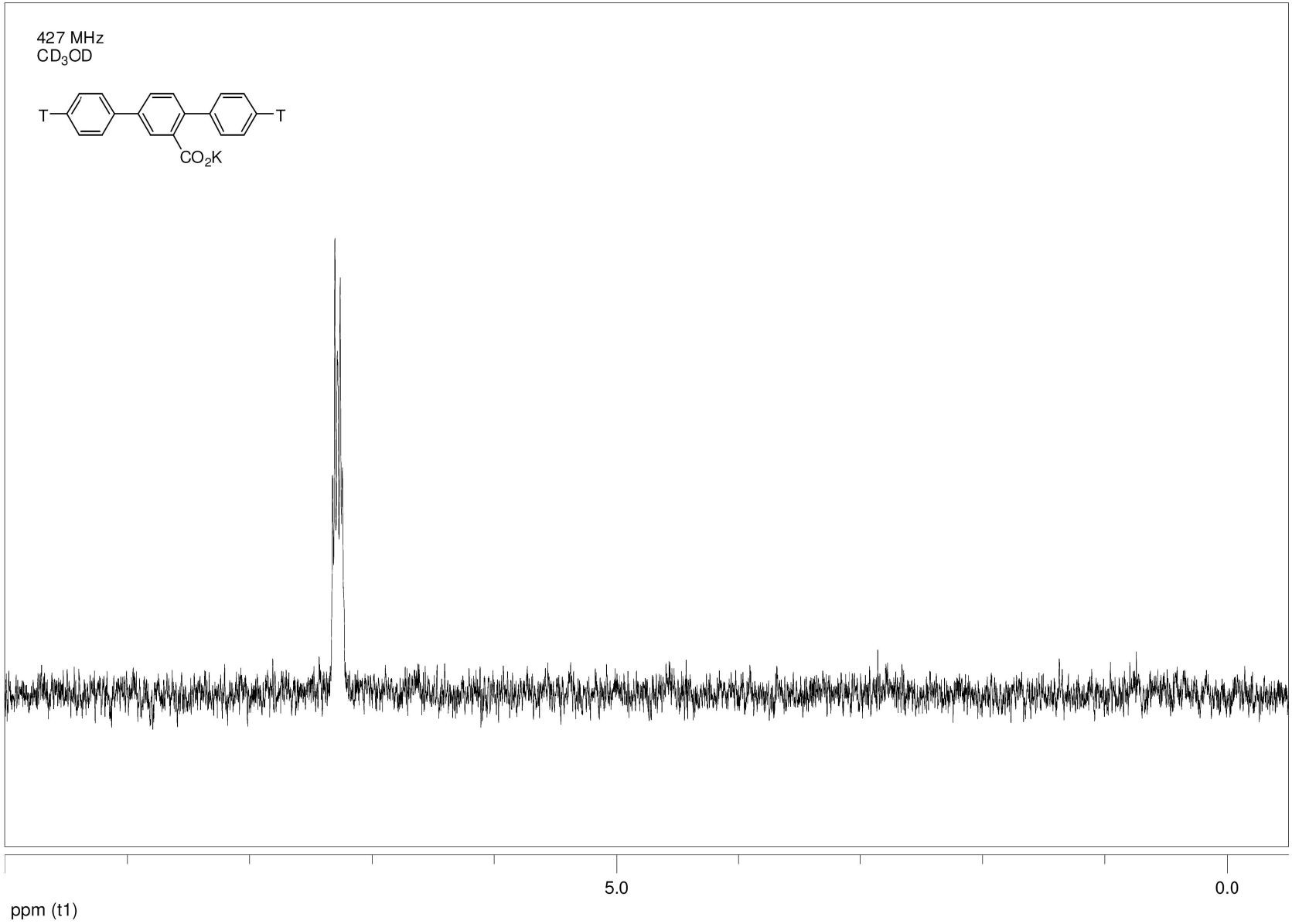
427 MHz
CD3OD
T
T
CO2K
5.0
0.0
ppm (t1)

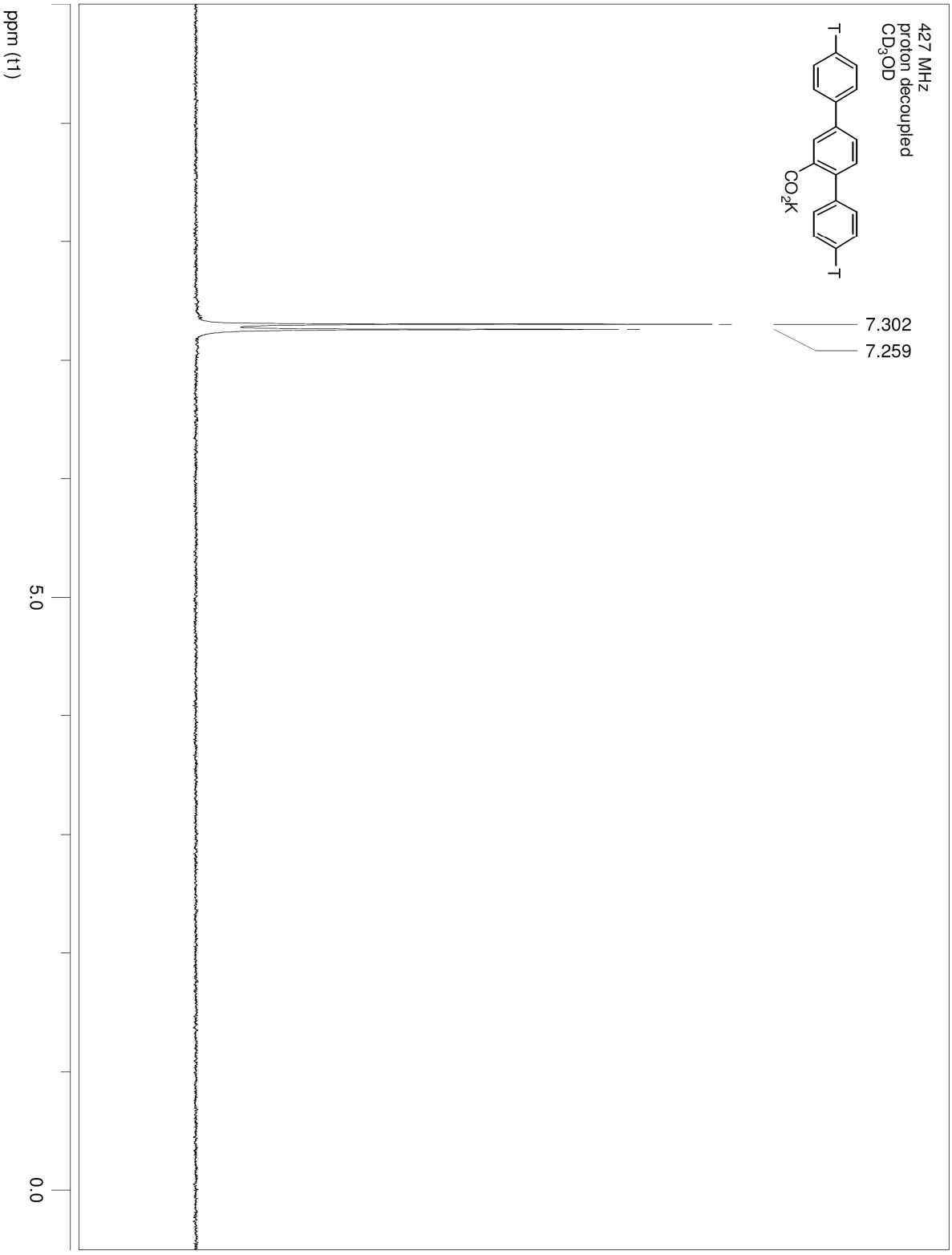
427 MHz
proton decoupled
CD_3OD
T
CO_2K
T
7.302
7.259
ppm (t1)
5.0
0.0

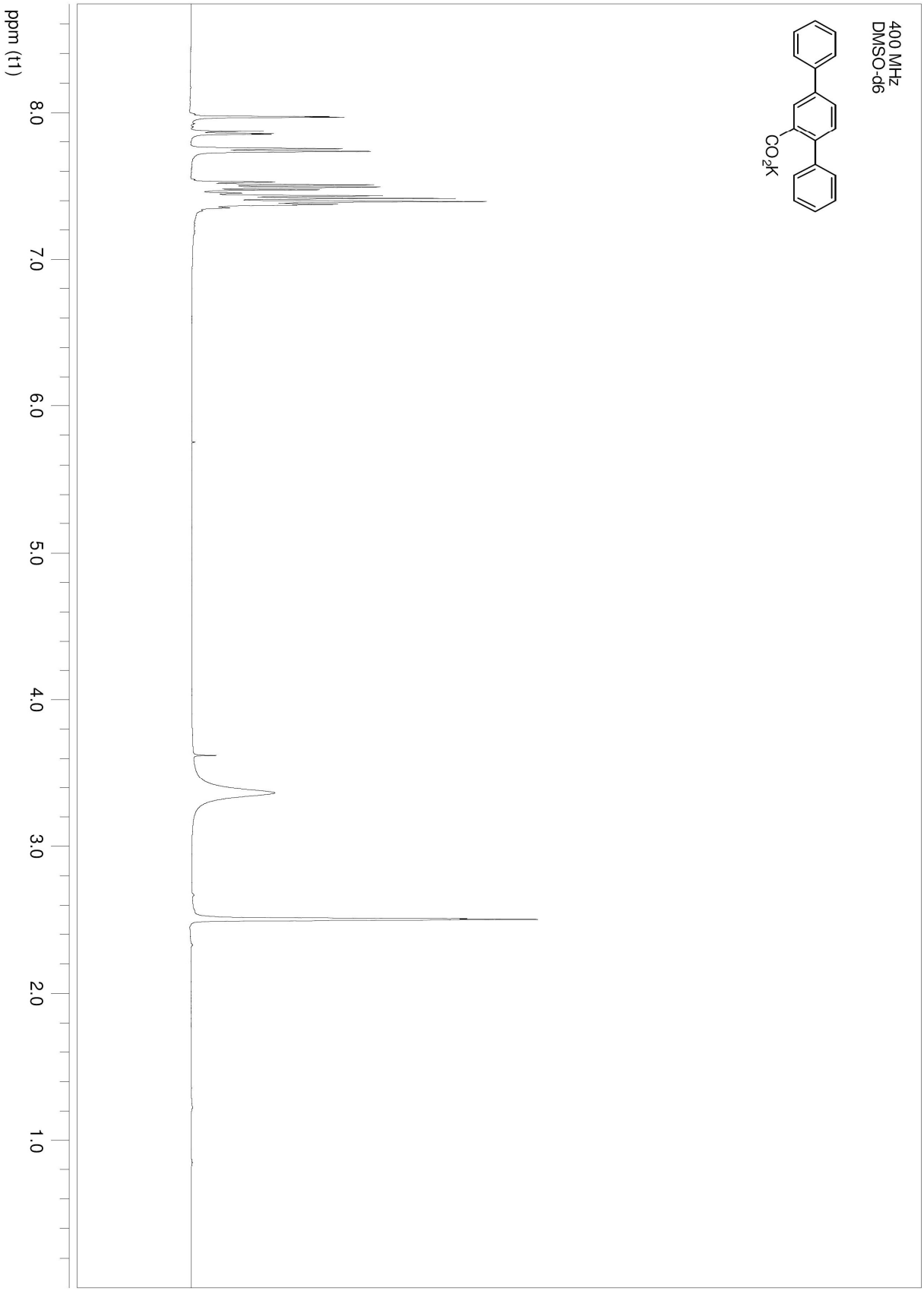
400 MHz
DMSO-d6
CO2K
ppm (t1)
8.0
7.0
6.0
5.0
4.0
3.0
2.0
1.0

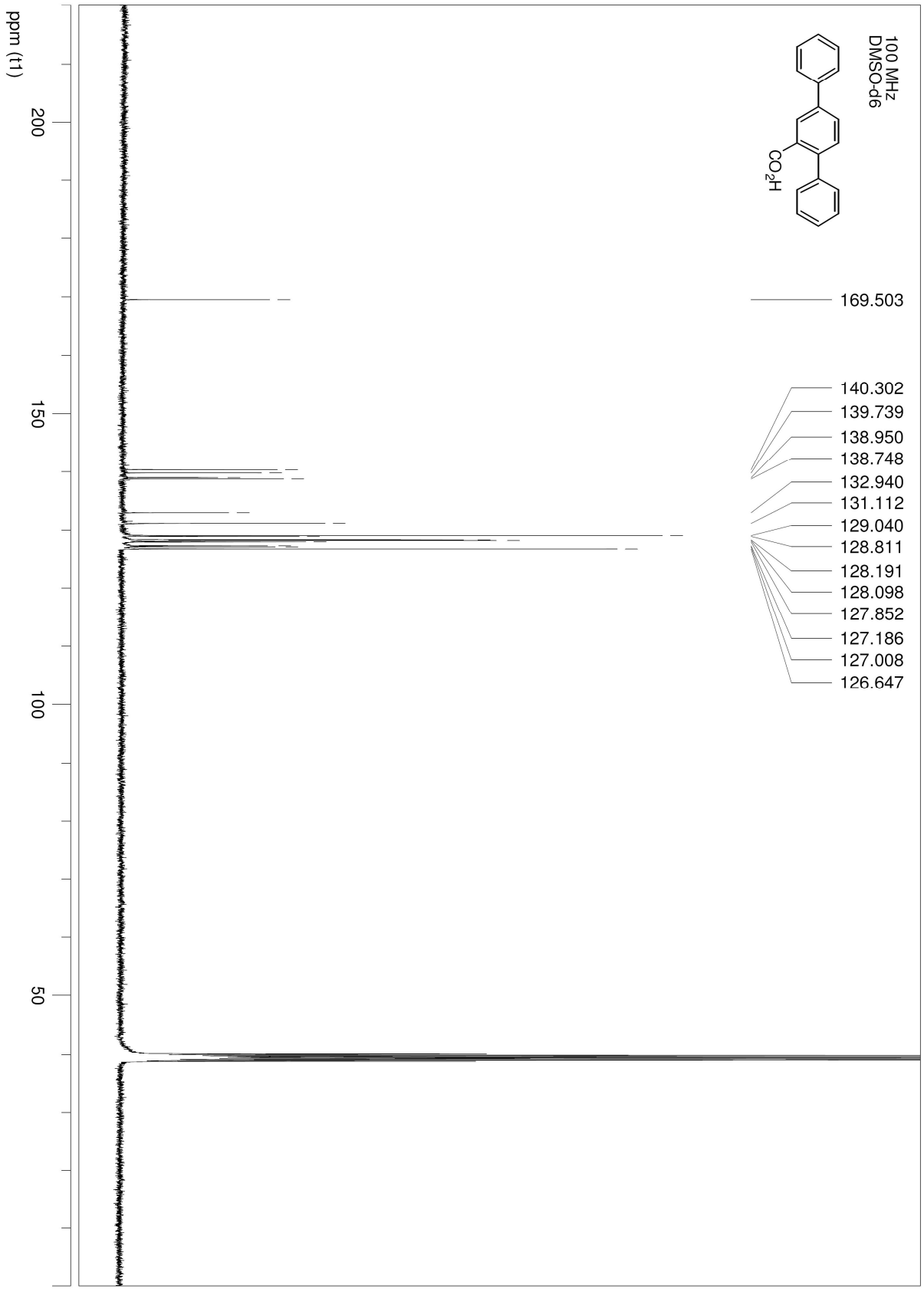
100 MHz
DMSO-d6
CO2H
169.503
140.302
139.739
138.950
138.748
132.940
131.112
129.040
128.811
128.191
128.098
127.852
127.186
127.008
126.647
ppm (t1)
200
150
100
50